INVESTGATION OF SAND EROSION OF PELTON TURBINE IN CHENANI HYDRO ELECTRIC PROJECT-I (5 x 4.66 MW)

A DISSERTATION

Submitted in partial fulfillment of the

Requirement of award of degree

of

MASTER OF TECHNOLOGY

in

ALTERNATE HYDRO ENERGY SYSTEMS

By

AMIT SHARMA

DEPARTMENT OF HYDRO AND RENEWABLE ENERGY
INDIAN INSTITUTE OF TECHNOLOGY
ROORKEE-247667 (INDIA)
JUNE 2019

DECLARATION

I hereby declare that the work which is being presented in this dissertation entitled **"INVESTIGATION OF SAND EROSION OF PELTON TURBINE IN CHENANI HYDRO ELECTRIC PROJECT-I (5 x 4.66 MW)."** in partial fulfillment of the requirements for the award of the degree of **Master of Technology** in **Alternate Hydro Energy Systems**, submitted in **Department of Hydro and Renewable Energy, Indian Institute of Technology Roorkee, Uttarakhand, India**, is an authentic record of my own work carried out under the supervision of **Dr. R. P. Saini**, Professor, Department of Hydro and Renewable Energy, Indian Institute of Technology Roorkee.

I have not submitted the matter embodied in this report for the award of any other degree or diploma.

Date: June, 2019
Place: Roorkee **(AMIT SHARMA)**

CERTIFICATE

This is to certify that the above statement made by the candidate is correct to the best of my knowledge.

Dr. R. P. Saini

Professor
Department of Hydro and Renewable Energy,
Indian Institute of Technology, Roorkee -247667

ABSTRACT

The erosion of hydro turbines through sand-laden river water is one of the biggest problems in the Himalayan region. Quartz is found as a major component in many of the Himalayan rivers, along with feldspar and other hard minerals, these particles have more than 5 hardness on Moh's scale, which can erode parts of hydro turbine. The problem of hydro-abrasive is usually seen in medium and high head turbines. In high head Run-of-River schemes, even small suspended sediment particles can cause severe hydroabrasive erosion particularly in Pelton turbine due to high impact on account of high velocity. Apart from jet velocity, erosive wear depends upon different parameters such as size, shape, concentration, mineral hardness and base material properties. When this water containing silt impinges on the bucket of the Pelton turbine through nozzle, erosion occurs which in turn results into efficiency drop, increase in maintenance cost and down time of turbine repair. Apart from runner of the turbine, parts which are usually affected due to hydroabrasive erosion are nozzle and its ring, spear and deflector. The erosion concern in hydraulic machines is expected to become more severe in the future due to higher availability of suspended sediments from retreating glaciers and heavy rainfall due to climate change.

The problem of hydro abrasive erosion is also observed in Run-of-River based Chenani hydroelectric project-I (CHEP-I, 5 x4.66 MW) located in the state of J&K under Jammu and Kashmir State Power Development Corporation. In the present study, the detailed study of the various components of CHEP-I have been done. The homogenous suspended sediment sample were collected from the forebay on a regular basis during the study period. The suspended sediment properties such as particle size distribution (PSD), suspended sediment concentration (SSC), shape and mineral composition were measured. In the laboratory, the samples were analyzed using the gravimetric method, laser diffraction, turbidity, Scanning electron microscope (SEM), X-ray diffraction (XRD), X-ray fluorescence (XRF) and Petrography. The erosion rate and efficiency reduction of turbine have been estimated using IEC-62364(2013) hydro-abrasive erosion model and correlations developed under earlier studies for High head ROR based hydropower plants. Erosion depth of different regions of the buckets such as Splitter height reduction, erosion in cut-out region and erosion depth in bucket outlet was estimated using IEC-62364 and it was found to be 1.51 mm, 2.10 mm and 0.55 mm respectively. Erosion rate of nozzle and efficiency reduction of Pelton turbine is also estimated by using correlations developed under earlier studies.

ACKNOWLEDGEMENT

I would like to express my sincere gratitude to my guide **Dr. R. P. Saini,** Professor, Department of Hydro and Renewable Energy, Indian Institute of Technology Roorkee for his valuable guidance, support, encouragement and immense help. I would also express my deep and sincere gratitude to **Dr. S. K. Singal**, Head, Department of Hydro and Renewable Energy, Indian Institute of Technology Roorkee for their motivation during the work of my dissertation.

Moreover, I am thankful to **Dr. Anant Kumar Rai**, Project fellow who has rendered selfless help and support in numerous ways during the course of study. I would remain grateful to all faculty members and staff of Department of Hydro and Renewable Energy, Indian Institute of Technology Roorkee and also would like extend my heartfelt thanks to all my family members and friends who have helped me directly or indirectly for the completion of this dissertation.

(AMIT SHARMA)

CONTENTS

LIST OF FIGURES

LIST OF TABLES

LIST OF ABBREVIATIONS

CHEP-I	Chenani Hydroelectric Project-I
HPP	Hydro-electric Power Plant
HVOF	High Velocity Oxy Fuel
IEC	International Electro technical Commission
IS	Indian Standards
JKSPDCL	J&K State Power Development Corporation Limited
LISST	Laser In-Situ Scattering and Transmissometry (a trademark of Sequoia Scientific Inc., USA)
PPM	Parts Per Million
PSD	Particle Size Distribution
ROR	Run-of-River
SEM	Scanning Electron Microscope
SSC	Suspended Sediment Concentration
TSS	Total Suspended Sediment
WC-CO-CR	Tungsten Cobalt Chromium
XRD	X-Ray Diffraction
XRF	X-Ray Fluorescence

LIST OF SYMBOLS

Symbol	Stands for	Units
C	Concentration of particles	ppm
de	Depth of erosion	mm
E_r	Erosion rate	mm/year
S_p	Silt particle size	mm
η_r	Efficiency reduction	---
dx	Volume-equivalent sphere diameter of particles, which is not exceeded by x % of their mass	μm
$d50$	Median diameter of graded particles	μm
$f\ (dp50)$	Particle size	μm
$f\ (\alpha)$	function of impingement angle α	degrees
K_{env}	Environment constant	---
K_f	Coefficient reflecting the flow pattern	---
K_{hardness}	Coefficient for particle hardness with respect to the hardness of the surface material	---
k_m	Coefficient for the material at the surface of a turbine part	---
K_{mat}	Material constant	-
K_{shape}	Coefficient for particle shape	---
K_{size}	Coefficient for particle size	μm
P	Exponent	---
RS	Reference size of turbine	mm
SSC	Suspended sediment mass concentration	Kg/m^3
V	Velocity of flow	m/s
V_p	Velocity of particle	m/s
vp	Relative velocity between a particle and the flow	m/s
w	Characteristic relative velocity [m/s] between the flow and the turbine part.	m/s
x	Exponent	---
Δt	Exposure period	h
δ	Abrasion rate	μm/hr.
η	percentage efficiency loss of rated efficiency	%

CHAPTER 1
INTRODUCTION

1.1 GENERAL

Hydropower is used as a principle source of energy in many countries as it is considered to be one of the cleanest source of energy. The total installed capacity in India is 49,382 MW and the share of units generated through hydropower is 1,35,539 GWh which makes 14.8% hydropower share of electric power installed capacity [1]. The future prospects in hydropower of Himalayan region are encouraging but the geological issue appears to be a significant barrier. The contribution of Asian rivers in terms of amount of suspended sediments in the World Ocean account for around 59% of the complete worldwide yield of suspended sediments. Nearly 70-90% of the annual sediment load is transferred in the Himalayan region during 14-24 days of the monsoon season due to intense seasonal rainfall, young geology and tropic climate [2]. Climate change adversely affects catchment run-off features resulting in an increased risk of severe flood and drought events. Climate change adversely affects catchment run-off features resulting in an increased risk of severe flood and drought events.

The two major challenges which Hydropower development encounters are (a) Loss of storage ability of reservoirs owing to the settling of suspended sediments on the ground and (b) Erosion of turbine components and hydraulic structures leading to power plant efficiency reduction. In India, total hydropower potential estimated at 845 hydropower sites (medium and large capacity) is about 148.7 GW to produce nearly 450 billion units of annual energy generation [2]. Himalayan region of India has about 80% of untapped hydropower and one of the major challenges for hydropower development, particularly for the Himalayan regions, is water transporting sediments in streams affects the lifespan and function of hydropower plants during high flow mainly composed of snow melting and rainy season. Hydroelectric plants operate during elevated stream, consisting primarily of snow melting and rainy season. The concentration of silt rises from 250 to 10,000 ppm and the particle size in the Himalayan streams exceeds 1000 microns during the monsoon season. The situation is aggravated if the silt includes a greater percentage of quartz, which is extremely hard and the level of quartz in Indian silt is extremely large. The issue of sediment handling, maintenance and operation of the power plants, particularly hydro turbines have become a matter of grave concern among Hydropower developers of Himalayan regions.

1.2 HYDRO TURBINES

It is a fluid device used to transform potential energy of water into mechanical energy and is then used in hydroelectric plants to run the generator for electricity generation. In addition, the hydro turbines are categorized into two classifications depending on stream path over the runner viz. impulse turbine and reaction turbine.

1.2.1 Impulse turbine

It is a type of turbine that is operated when high-velocity water jets are aimed from a nozzle to the buckets attached to a wheel. Before entering the turbine, the fluid pressure head is converted to the velocity head by passing the fluid through a nozzle. The water coming from the jet strikes the blade at high speed which rotates the rotor. The kinetic energy of water is transferred to rotor which is coupled with generator with the help of shaft to rotate the generator and after transferring energy, water flows to the tail race. The casing has no hydraulic role in developing power but it is provided only for avoiding the splashing of water in powerhouse and guide the water to tailrace in order to protect the bearings and other equipments housed in the powerhouse building. Examples of impulse turbines are Pelton turbine, Turgo-impulse turbine and Crossflow turbine.

(i) Pelton turbine

In the 1870s, the American engineer L.A. Pelton discovered the Pelton turbine. It is a tangential flow impulse turbine where potential energy available in water at inlet is fully converted into kinetic energy before water enters the turbine runner. The runner is made up of a metallic disc where a number of buckets are attached on the periphery of the disc as shown in Figure1.1.

In this turbine, the jet has to strike over a single bucket at a time as shown in Figure 1.2. The energy available at the outlet for the Pelton turbine is kinetic energy. At the turbine inlet and outlet, only atmospheric pressure is available. Pelton turbines are usually considered for heads more than 150 m, a higher running speed for micro-hydro applications. The main components of Pelton turbine are runner buckets, nozzle system which includes spear and seat ring, deflector and its casing. It is provided with a breaking jet that operates when the water hitting the runner of the buckets decreases to zero owing to inertia, but it continues rotating for a long time. A small nozzle is provided that directs the water jet on the back of the veins to stop the runner in a short time.

Figure 1.1: Runner of a Pelton turbine [3].

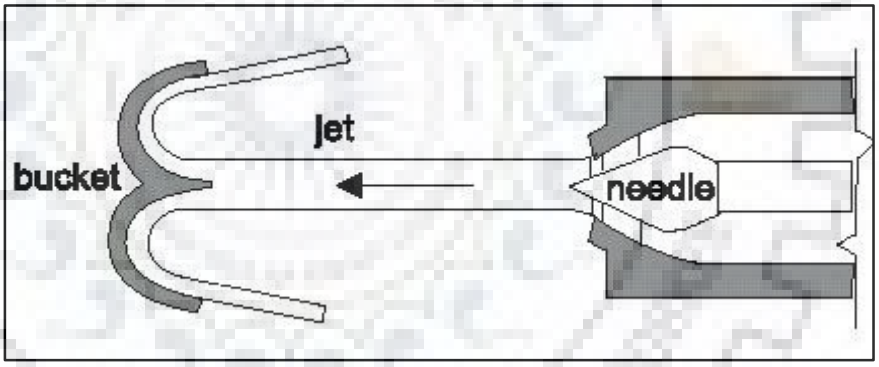

Figure 1.2: Water jet coming out of nozzle striking bucket [4].

(ii) Turgo impulse turbine

It is basically an impulse type turbine like Pelton turbine where water through nozzle strikes over the runner. The runner consists of number of buckets between two rims as shown in Figure 1.3 (a). The bucket is of cup shaped without having the splitter i.e. cup is simple in shape. The water from jet enters at the periphery of runner over the bucket from one side and comes out another side from the bucket as shown in Figure1.3 (b). In this turbine, a single jet strikes number of buckets (mostly three buckets) at a time. However jet does not lie in the same plane of runner.

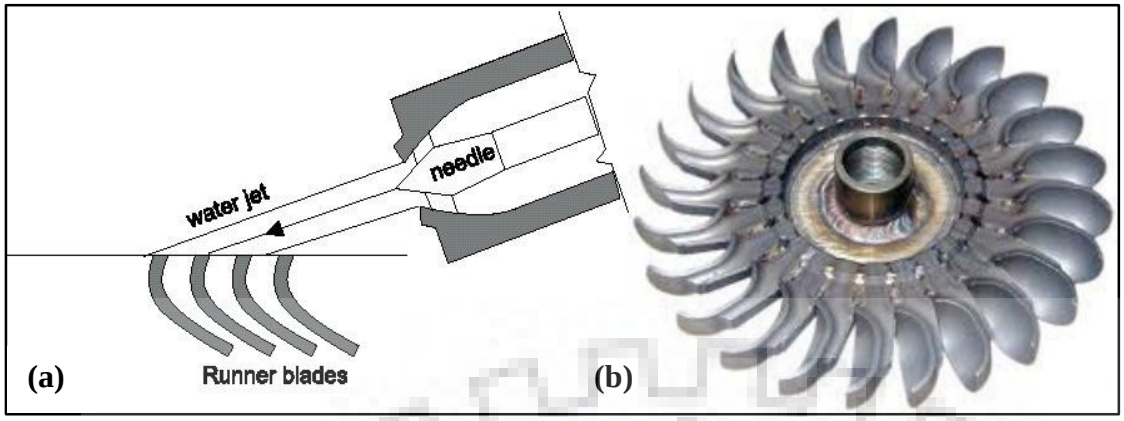

Figure 1.3: Turgo-impulse turbine (a) Position of jet with respect to runner blades b) Turgo Runner [5].

(i) Crossflow turbine

It is also an impulse type turbine, the shape of runner is entirely different which is of drum shape where number of curved blades are attached between two discs around the shaft as shown in Figure 1.4. The water jet over the runner strikes on the first stage of the curved blades crosses the shaft and strike again over the blades in opposite side and then leave the runner as the water crosses the shaft in the runner. In the Crossflow turbine, the nozzle is rectangular in shape and it covers one-fourth of the periphery of the runner. This turbine is also known as Banki turbine or osberger turbine where the energy transformation takes place at two stages from water to runner. It is recommended for microhydel only as it has low efficiency.

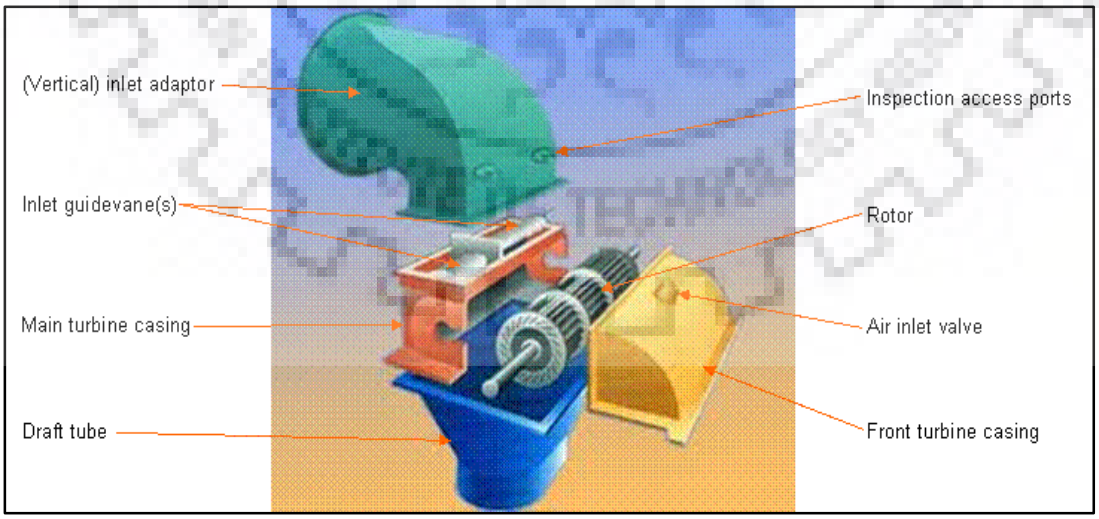

Figure 1.4: Main parts of Crossflow turbine [5].

1.2.2 Reaction turbine

The force of water pressure is applied on the face of runner blades and pressure decreases when it proceeds through the turbine rotor blade. The fluid pressure changes as it moves through the turbine rotor blades. It operates with its runner submerged in water. In this type of turbines, pressure and kinetic energy are available before the water entering the turbine. The reaction turbine is further classified into main categories based on the flow direction of water in the runner as mixed flow and axial flow turbine. In case of mixed flow turbine water enters from outer periphery of the runner moves in radial direction and comes out from centre in axial direction.

(i) Francis turbine

It has a runner with fixed blades (vanes), to which the fluid, with respect to the shaft, enters the turbine in a radial direction and exits in an axial direction. The main components comprise of the runner, a volute casing to pass the water to the runner, wicket gates or guide vanes to control the quantity of water and distribute it equally to the runner and at the end, a draft tube to convey the water from the turbine side to tail race as shown in Figure 1.5.

It is a closed type of turbine where pressure varies from inlet to the outlet of turbine. Therefore, it has volute casing as to maintain the velocity of water constant along the runner which can be explained as at the inlet of turbine all the quantity of discharge enters in the turbine accordingly flow area is determines as large. However when this water flow around the runner a quantity of water continuously flowing through the runner. Hence from starting to end point of the runner is continuously decreasing, accordingly cross-section of the area is required to reduce to maintain the constant flow velocity.

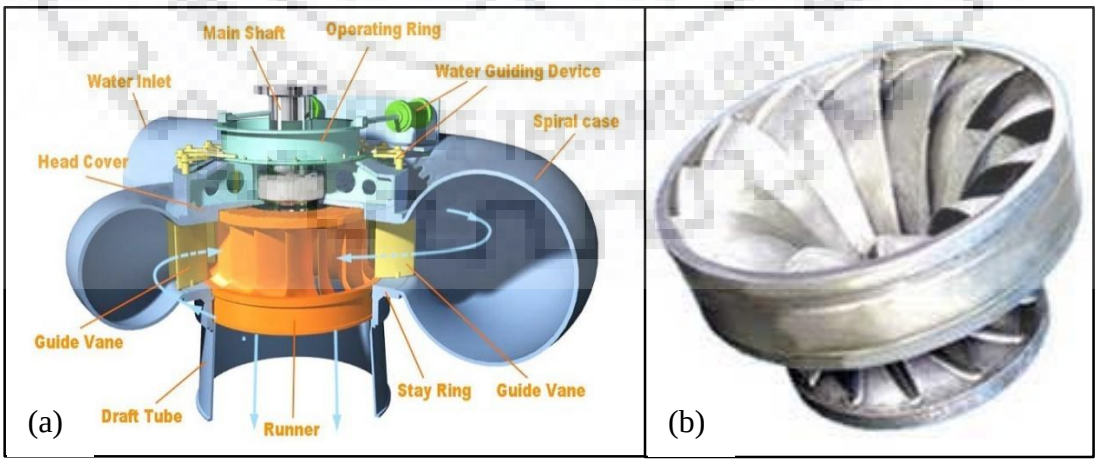

a) Main components **b) Runner**

Figure 1.5: Main parts of Francis Turbine [5].

In case of axial flow turbines, water enters form the wicket gate to the runner in axial direction, moves along the runner and comes out in axial direction. Axial flow turbines utilizes low head where large volume of water is available. These turbines provide large flow areas and run at very low speeds. Axial flow turbines are classified based on operating conditions as propellor turbine, Semi Kaplan turbine and Kaplan turbine. The main parts of Kaplan turbines are shown in Figure 1.6.

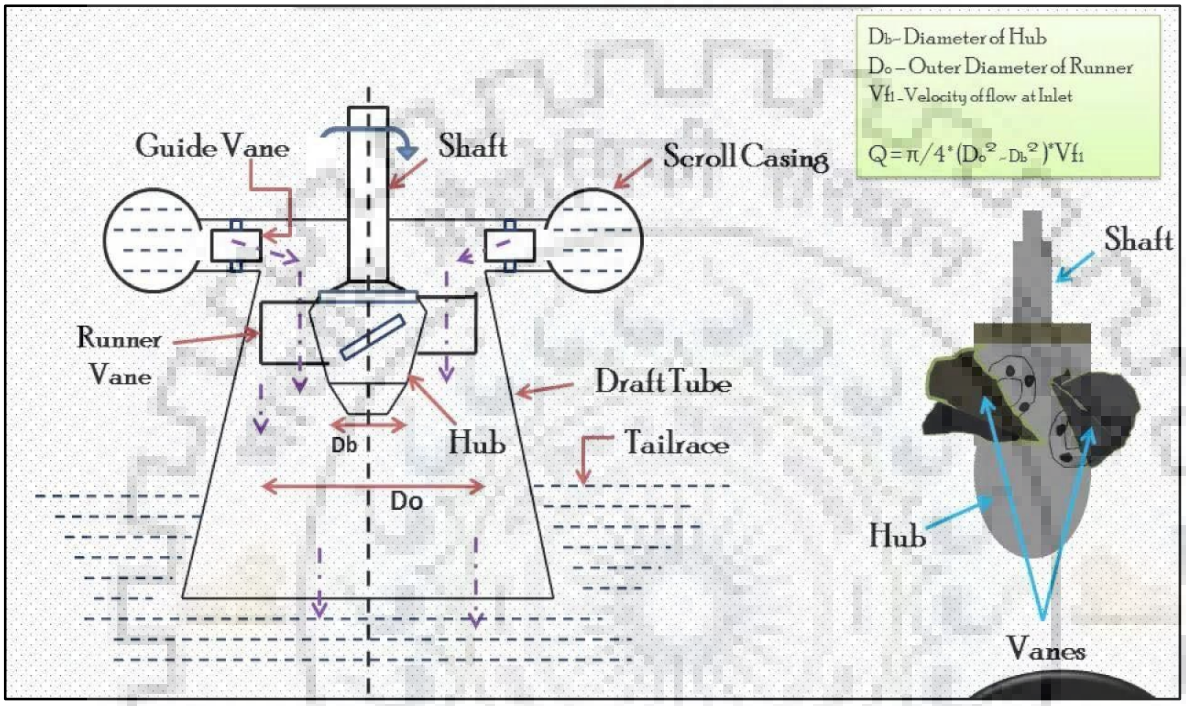

Figure1.6: Main parts of Kaplan Turbine [6].

1.3 FACTORS AFFECTING THE EFFICIENCY OF HYDROTURBINE

There various reasons which affects the efficiency of hydro turbine is owing to various reasons are (i) leakage of water without doing useful work (ii) friction loss due to roughness of the surfaces. Erosion in turbines occurs due to several reasons which in turn reduces the efficiency of the turbines. The highest efficiency loss in case of Pelton turbine occurs at best efficiency points. The efficiency loss in eroded turbine is due to effect of following reasons [7]:

i. Water loss through erodent entrance lips.
ii. Change in directions of blades due to erosion at outlet edge of bucket and braking effect of back fitting.

The damages in hydro turbines are mainly due to sand erosion, cavitation, material defects and fatigue.

1.3.1 Cavitation

It is phenomenon which occurs during operations of a hydraulic turbine and is undesired condition. It is the formation and collapse of vapour cavities in a flowing liquid. It can form anywhere in the flowing liquid. The formation of the vapour takes place where the local pressure is less than the liquid vapour pressure at corresponding temperature and collapse of bubble will begins when they are moved into regions where the local pressure is higher than the vapour pressure i.e. Whenever pressure in the liquid drops below the vapour pressure corresponding to its temperature, the liquid will vaporize. The micro jets hits the surface of the turbine and pitting takes place.

1.3.2 Sand erosion

Sediment has been defined generally as solid particles which are moved or might have been moved by flow in channel. Sediments are mainly considered as products of disintegration and decomposition of rocks. The sediments found in river are mixture of different particle size. Turbine erosion is basically caused by sand fraction of the sediment [7]. Sand fraction divided into fine (0.06-0.20 mm), medium (0.2-0.6 mm) and coarse (0.6 -2 mm). Sand erosion of turbines results in mechanical wear of turbine components due to dynamic action of sediment flowing along with water. However the mechanism of erosion is complex process due to interaction of various reasons such as particles size, shape, hardness, concentration, velocity, impingement angle and base properties of material [7]. There are several other factors, which distinguish types of erosion mechanism and control erosion rate. The major problems faced in Pelton turbine are the damages of their runner buckets and nozzle system (spear and seat ring) due to cavitation and due to sand erosion. The sediment laden water passing through the turbine is the main cause of hydro-abrasive erosion of turbine components resulting in loss of efficiency thereby frequent shutdown of plants, vibrations in machine, failure of machine unit due to mechanical reasons, abetting of cavitation, pressure pulsations, mechanical failures. As hydro-abrasive harm is caused by the continuous action of the sediment characteristics with the component, therefore, mechanical properties of the component in contact with the flow and flow conditions are simultaneously responsible for the intensity and amount of silt erosion. The effects of hydro-abrasive erosion in turbines is shown in Figure 1.7.

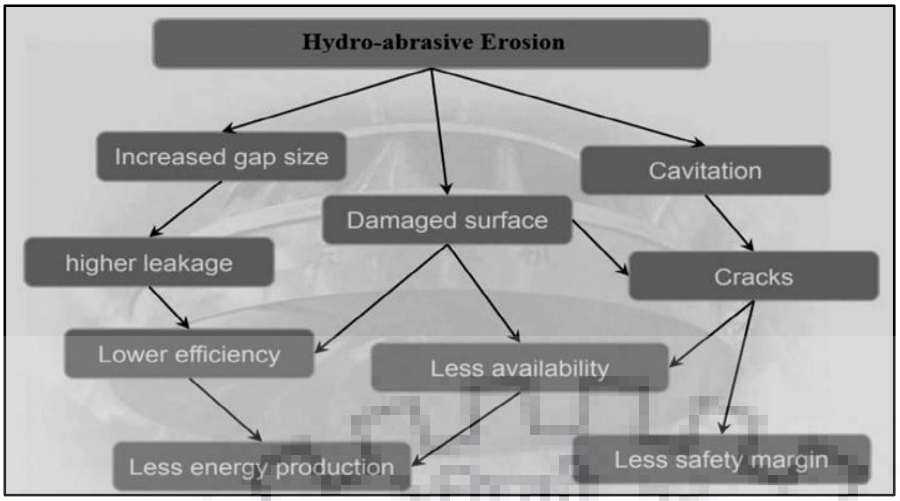

Figure1.7: Effect of Hydro-abrasive erosion in turbines [8].

Hydraulic machines operating under medium and high heads are usually exposed to erosion. High head Francis and impulse turbines are extremely affected by sand erosion. In rivers with high sediment content, even low-head Kaplan turbines and propeller turbines are also found to be eroded. Both sand erosion and cavitation reduces the performance of turbine which in turn results in decreasing the efficiency of the turbine. It also contributed to increase the generation cost of the power plant due to frequent breakdowns. The life of the turbine components also gets reduced as sand erosion disturbs the profile of the components.

1.4 FACTORS AFFECTING THE SAND EROSION

1.4.1 Operating conditions

Velocity, acceleration, impingement angle, flux rate or concentration, medium of flow and temperature are the main operating conditions in turbine. However velocity and impingement angle play an important role and it is the factor which is associated with the erosion of turbines. It is seen in every erosion model related to hydraulic turbines.

1.4.1.1 Velocity of Erosive particle

The most used expression to describe relation between erosion and the velocity of particle is given in Equation (1.1).

$$\text{Erosion} \propto (\text{velocity})^{m} \qquad (1.1)$$

The erosion is often considered proportional to the velocity raised to an extent m. Most reference gives value of m between 2 and 4. Different investigator use different value for their erosion model. Different investigator use different value for their erosion model. However IEC guideline suggests to take the value of m as 3.4 [9]. The velocity which is used for

calculation is the characteristic relative velocity between the flow and turbine and is measured in metre per second.

1.4.1.2 Impingement angle

Impingement angle is the angle between the eroded surface of the bucket and the trajectory of the sediment particle just before the impact. Normally jet angle is considered as impingement angle for practical purpose which is not true. If the sediment particles are moving parallel to the surface of the turbine component, impingement angle is considered as 0° and hence only minor erosion may take place. When these sediment particles are moving perpendicular to the surface of the impingement angle is considered as 90°. It differs from zero degrees to ninety degrees.

1.4.2 Eroding particles

The characterstics of sediment particle flowing through turbine decides the pattern of erosion mechanism and erosion rate. Therefore it is important to have good knowledge of these particle characterstics in order to estimate, reduce and prevent erosion. The characterstics and their effects are discussed below.

1.4.2.1 Concentration

Concentration is one of the important property of sediments and mainly erosion rate is considered proportional to concentration. It defined as mass (or volume) of particle present in unit mass (or volume) of fluid. It can be represented in terms of percentage of particles in a given fluid mass (or volume). Concentration is also presented in the form of PPM (parts per million) particularly in case of river sedimentation, which is equivalent to mg/litre or kilogram of particle in $1000m^3$ of water (1000 ppm is equivalent to 0.1 %).

1.4.2.2 Particle size

As distinct particle sizes have different actions in a fluid stream, this has an impact on the turbine components of their type of deformation. Particle size can be characterized mainly by mass and length in two fundamental sizes. The kinetic energy of particle for a specified velocity is directly proportional to mass. The spherical particle mass is equal to $(diameter)^3$. Therefore, the particle size is determined by determining the diameter of the particle.

1.4.2.3 Particle shape

The Particle shape is considered as one of the important factors responsible for erosion rate. Apart from erosion rate, the particle shape of eroding particles are of great interest as it has influence in shear strength, density, permeability, compressibility and capacity of sediment transport. Normally particle shapes are described qualitatively such as round, sub angular and angular based on visual observation. International electro technical (IEC) commission suggests to take the value of shape factor (k_{shape}) for erosion as 1, 1.5 and 2 for round, sub-angular and angular particles respectively [9].

1.4.2.4 Particle hardness

The shape and hardness of particle compliment to each other. It has been observed that even hard particle but relatively low blunt shape may not cause severe erosion. Hard particles tend to have shape profile; in contrast, edges of soft particles round off even with slight impact. Severe erosion occurs if the particles are harder than substrate. But if particles are softer, erosion occurs only if the substrate has low fracture toughness. Hence the ratio of hardness of the particle and substrate is very influencing in determining erosion rate. Normally Mineral hardness of the particle is represented in relative term of Moh's hardness scale between 1 for chalk powder to 10 for diamond [10]. Hardest mineral present in sand is quartz which has hardness of 7 on Moh's scale.

1.4.3. Base material properties

The turbine components which are exposed to high velocity should have material property such as higher yield stresses, improved fatigue life, cavitation and corrosion resistance. The turbine material should have less weight per generation capacity. Erosion is usually not considered when material of turbine is selected.

1.5 EROSION IN PELTON TURBINE

Pelton turbine is an impulse turbine which operates under high head. In Pelton turbine, all the available potential energy of water is transformed into kinetic energy with the help of nozzle placed before the water enters turbine, the turbine is connected to generator through shaft which rotates when the turbine is rotated and then generator starts generating electricity.

During this process, force is exerted by sediments present in water on the turbine parts resulting in deformation of turbine components. The jet velocity is usually very high because of high head application of Pelton turbine. Since velocity is the dominant factor for erosion as erosion $\propto (\text{velocity})^3$. Thus high velocity of flow makes flow turbulent which in turn brings

the dimensional change of the components leads to efficiency loss and eventually the failure of system. Runner buckets, splitter, spear, seal rings in the nozzles, are prone to sand erosion and gets eroded as shown in Figure (1.8), Figure (1.9) & Figure (1.10) respectively.

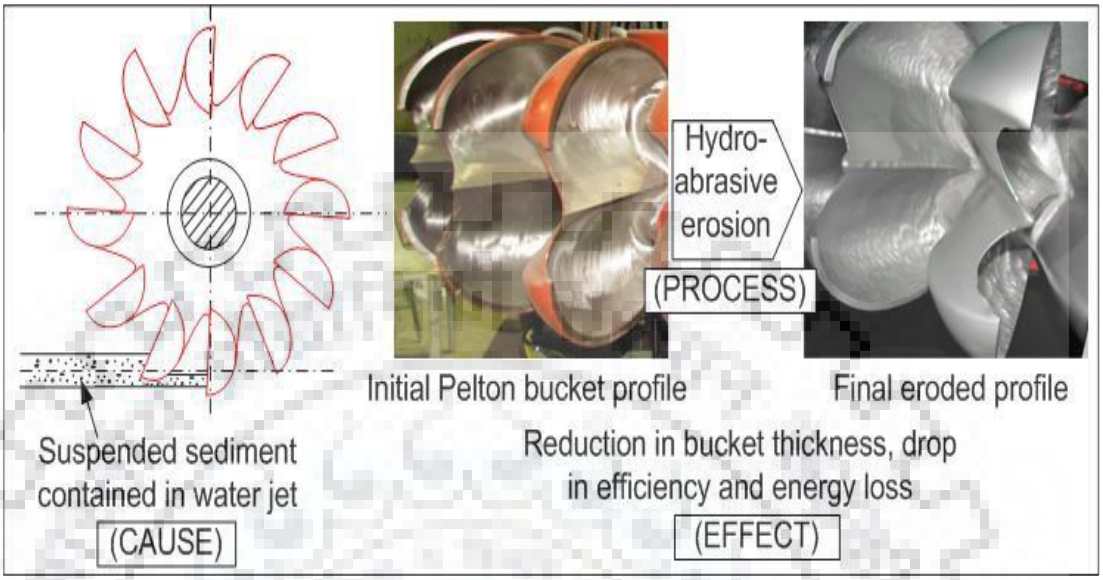

Figure1.8: Hydro abrasive erosion on Pelton Runner [12].

Figure1.9: Damaged buckets of Pelton wheel of CHEP-I.

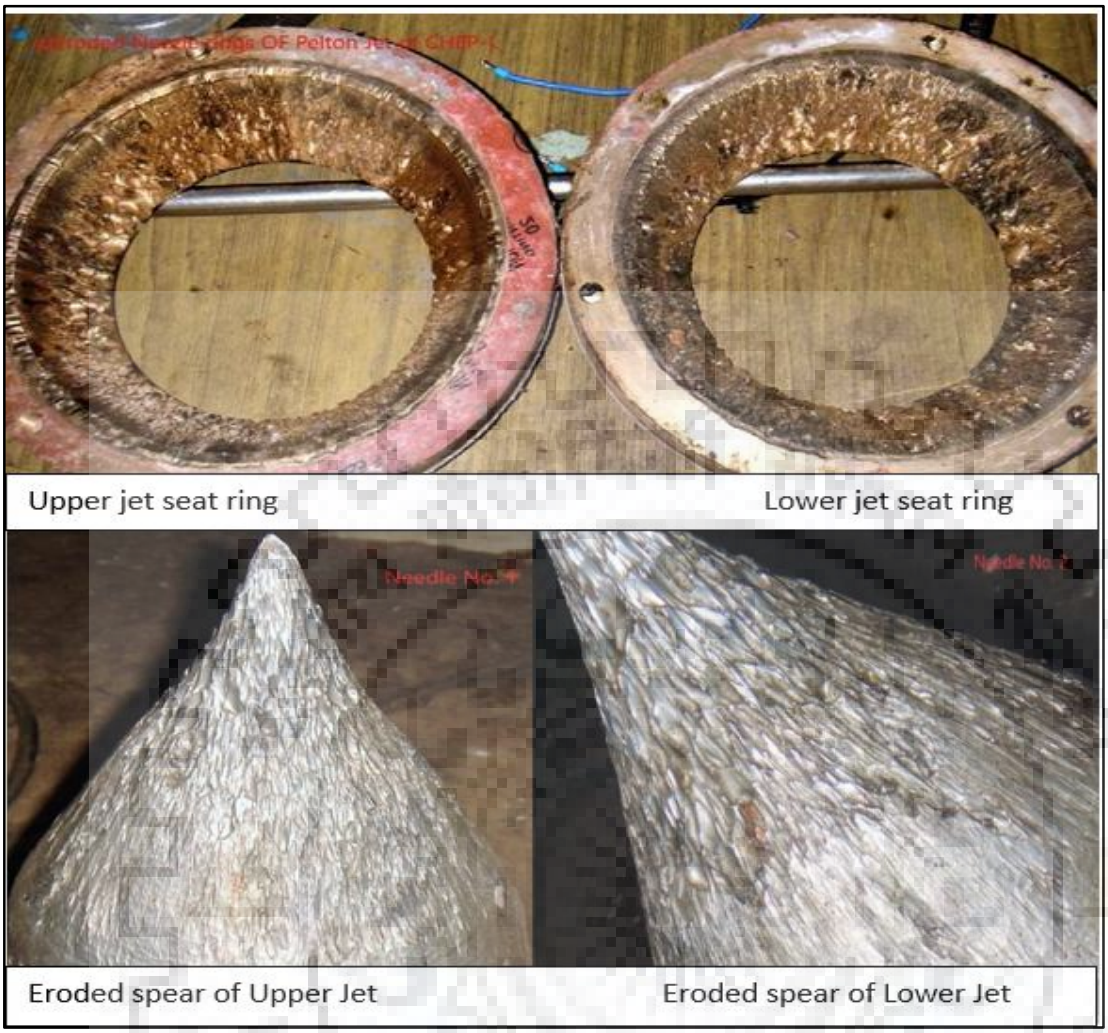

Figure 1.10: Severely Eroded Nozzle system (spear and seat rings) of twin jet Pelton Turbine of CHEP-I.

1.5.1 Erosion in nozzle system

When the suspended sediments along with water passes through the nozzle system at high velocity, then erosion of nozzle system occurs. The operating conditions decide erosion pattern and erosion intensity of nozzle system. During the full opening of the needle or spear, the continuous water is withdrawal from the nozzle so the mean speed increases along the surface of needle which in turn decreases the pressure on force towards the needle tip. Although velocity is maximum towards the tip, but the force at this point is minimum, which decreases the intensity of the erosion in this region. The erosion pattern is looked as ripples with circular grooves when it is viewed in axial direction. When the needle is partially opened, the contraction of the fluid passage increases further, which reduces the pressure to such an extent that it can give rise to cavitation. In this case, a combined effect of erosion and cavitation can be seen on the needle surface. The erosion patterns of full and partial opening of needles is shown in Figure 1.11. Beside needles or spears, the outer seat rings of the nozzle also faces

similar erosion problems.

In summary, one of the most eroded components of Pelton turbine is the nozzle system due to a highly turbulent flow. The erosion intensity of needle becomes more severe during the part load operating conditions due to the combined effect of erosion and cavitation. The challenges of sediment erosion in the nozzle system cannot be solved by a hydraulic design, but it can be minimized using hard base material for nozzle system and by applying hard coating over needle surface.

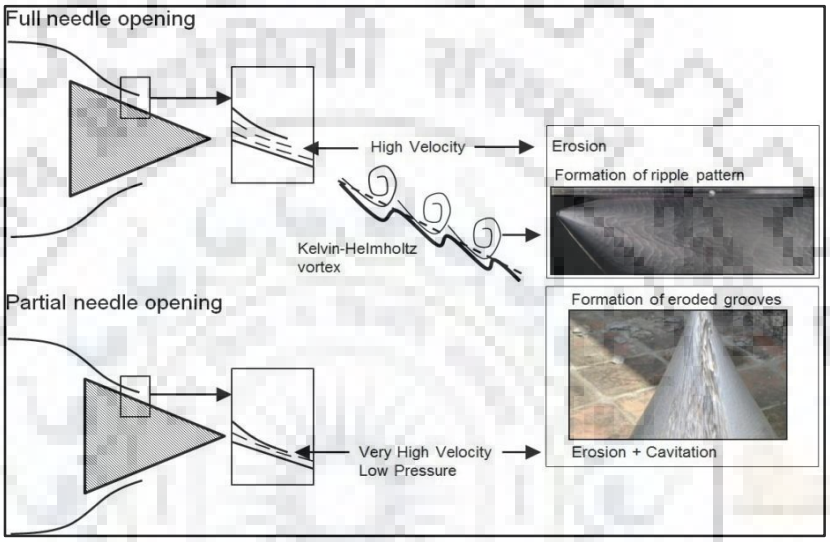

Figure1.11: Erosion patterns of needle in full and partial opening [12]

1.5.2 Erosion of Pelton runner

The rotating part of the Pelton turbine is runner. The number of buckets evenly spaced are fixed on the periphery of circular disc. Two hemispherical bowls are joined together to make buckets. Each bucket have a wall in between two hemispherical bowl called splitter. The job of the splitter is to splits the jet of water striking the buckets into two equal parts and the jet of water comes out at the outer edge of the bucket. The buckets are designed in such a way that the jet of water strike the buckets it gets deflected through 160 degree to 170 degree. The Pelton turbine buckets made up of cast iron, cast steel bronze or stainless steel. The different components of Pelton turbine bucket is shown in Figure1.12 (a) and Figure 1.12(b) shows the hot spots created on the bucket of turbine.

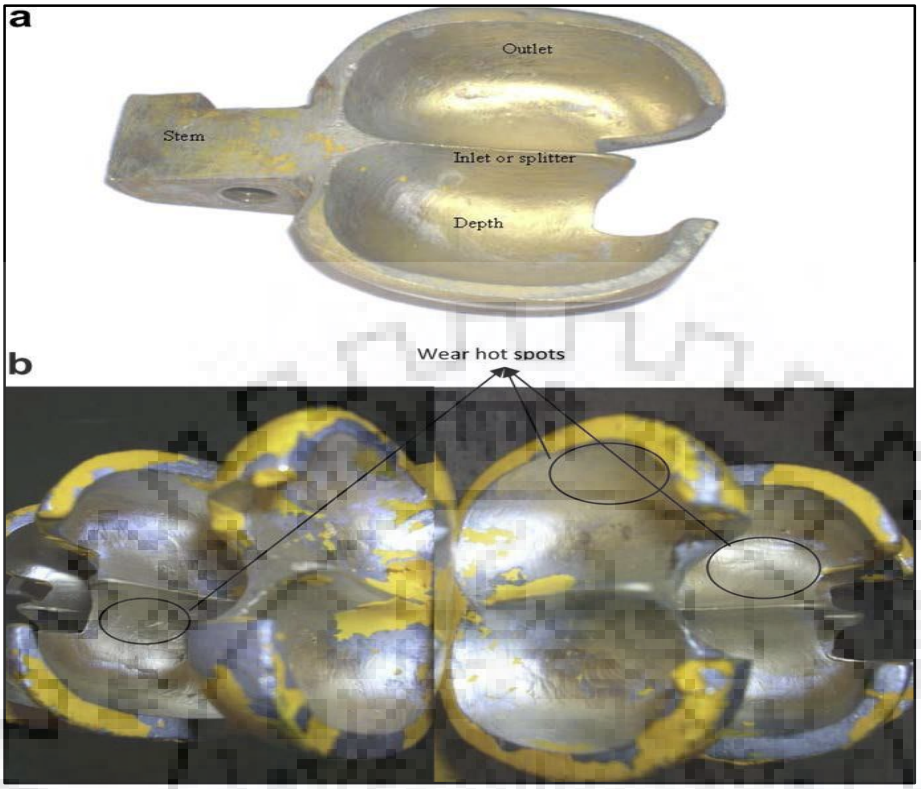

Figure 1.12: (a) Different components of the buckets of Pelton turbine. (b) The marked areas as wear hot spots on the bucket [13].

It has been observed that the suspended sediment along falls normal to bucket with a very high acceleration due to which the sediment particles gets separated from the flow and collide on the surface of Pelton bucket. It has been shown that the erosion in the bucket of Pelton turbine is sensitive to its curvature (R). The location and type so for erosion have been classified is according to the size of the sand particles [14]. The coarse particles most likely hit the bucket inlet, eroding the surfaces around splitter. Fine particles glide along with water and strike on the outlet surface. It was also seen that the damages in the splitter and entrance lip were severe due to direct hitting of the particles. The erosion on the surface of the bucket on the other hand, was seen like a hammering effect. It has also been explained that the loss in efficiency in Pelton turbines is mainly due to the erosion of the entrance lip. Erosion is usually most severe on leading edges, i.e. on splitter crests and at cut-outs of Pelton buckets [13]. Figure1.13 explains the particle separation at high acceleration inside the bucket and the different erosion patterns due to different sizes of materials hitting the bucket.

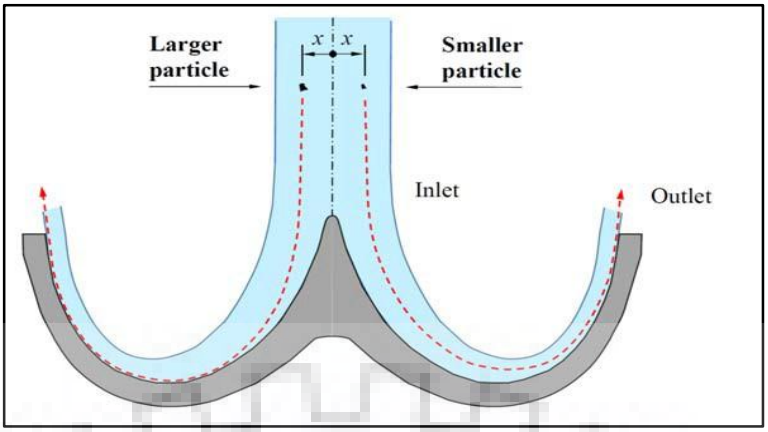

Figure 1.13: Particle separation at high acceleration inside the bucket [14].

1.6 OUTLINE OF DISSERTATION

The dissertation work in this report is presented in six chapters as follows:

i. Chapter 1: the different types of hydro turbines are discussed along with factors affecting the efficiency of turbines. The issue of hydro-abrasive erosion in Pelton turbine is also discussed under this chapter.

ii. Chapter-2: an extensive literature is reviewed related to sand erosion of turbines. Investigations of sediment parameters and erosion models developed by various researchers reported in literature are discussed.

iii. Chapter-3: the study of various components of chenani hydroelectric project-I are discussed in detail. All primary and secondary data from the site have been collected.

iv. Chapter-4: the various instruments and techniques required to measure the sediment properties like concentration, size, shape and mineral hardness are discussed. The details of samples collected manually from the forebay of CHEP-I during the month of June, July, August and September 2017 are also provided .The sediment properties are measures and analyzed in this chapter. Available erosion models like IEC-62364 and available correlations are studied and used to estimate erosion rate and efficiency reduction of Pelton turbine installed at case study power plant, chenani hydroelectric project-I. The analyzed sediment parameters and erosion models readings are recorded and results are obtained. The estimated erosion rate obtained from erosion model are discussed and then compared with erosion rate measured at site.

v. Chapter-5: based on results and discussions, conclusion is drawn and recommendation of further work is presented.

CHAPTER 2
LITERATURE REVIEW AND OBJECTIVE OF THE STUDY

2.1 GENERAL

Hydro-abrasive erosion in hydro turbines has become a complex phenomenon as it depends on sediment properties such as concentration, particle size, particle shape and mineral hardness. Apart from sediment parameters, base material properties and velocity are also the factors responsible for erosive wear of hydro turbine. High concentrations of harmful silt and fine sand particles are typically found in the turbine water of Run-of-River power plants using water originating from catchment areas with high specific sediment yields. High sediment yields are typical for currently or formerly glaciated catchments and relatively young geological formations, and are reported from the Himalaya. In many of these areas, the percentage of hard minerals such as quartz and feldspar is relatively high.

During monsoon, it becomes impossible to control these sediments and when they pass through turbine components, erosion occurs. Erosion in hydraulic machines causes (i) increased roughness on parts in contact with the water and (ii) degrades their shapes, i.e. the so-called hydraulic profiles. This leads to reductions in efficiency and may affect the mechanical stability and integrity of machine parts. In order to maintain hydraulic machines in good condition, frequent maintenance and repair works as well as replacements of eroded parts are required. This results in increased costs as well as in losses in electricity generation and revenues due to reduced efficiency and downtimes during works. The effect of sediment-laden water in the hydraulic machinery is basically aimed to contribute the knowledge for: (i) operational strategy of hydropower plants (ii) selection and design of turbine components (iii) selection of appropriate material for turbine construction and maintenance (iii) maintenance of eroded turbine and maintenance scheduling. Therefore, it becomes necessary to investigate the effect of sand erosion in turbines. Under this Chapter -2 an extensive literature related to sand erosion in various components of hydro turbines and erosion models developed by the various researchers to estimate erosion rate and efficiency reductions of hydro turbines are discussed.

2.2 HYDRO-ABRASIVE WEAR

The hydro-abrasive erosion is a complex phenomenon depending on many factors which can be broadly clustered in three groups (a) operating conditions, i.e. velocity, acceleration, impingement angle, type of fluid, temperature; (b) sediment parameters properties i.e. Particle concentration, Particle shape, Particle size, Mineral hardness, mineral composition; and (c) substrate (target material) properties, i.e. elasticity, hardness, surface morphology [15]. Wear

of Hydro turbine due to sediment erosion, denoted as erosion, is one of many types of wear. Wear is defined as (ASTM G40 - 88) "damage to a solid surface, generally involving progressive loss of material, due to relative motion between that surface and a contacting substance or substances ". Bhushan [16] recognised six principal wear mechanisms, which are quite different phenomenons, but have only one thing in common, that is 'removal of solid material from rubbing surfaces'.

The effect of erosion can be seen in a wide range of machinery within power, aviation, process and mining industry. The parts of hydro turbines and other components of hydropower plants are eroded due to sand in water. Water jet machining, sand blasting, erosive drilling and rock cutting are some good examples of beneficial application of erosion mechanism. Mechanical, chemical and thermal actions are the main cause of material separation as debris in erosion, but means for reaching those actions are different. The four basic mechanisms for solid particle erosion are Cutting, fatigue, brittle fracture and melting. Cutting actions can also be divided into; cutting by penetration of cutting edge or plastic deformation to failure. The hierarchy of these processes is shown in Figure 2.1.

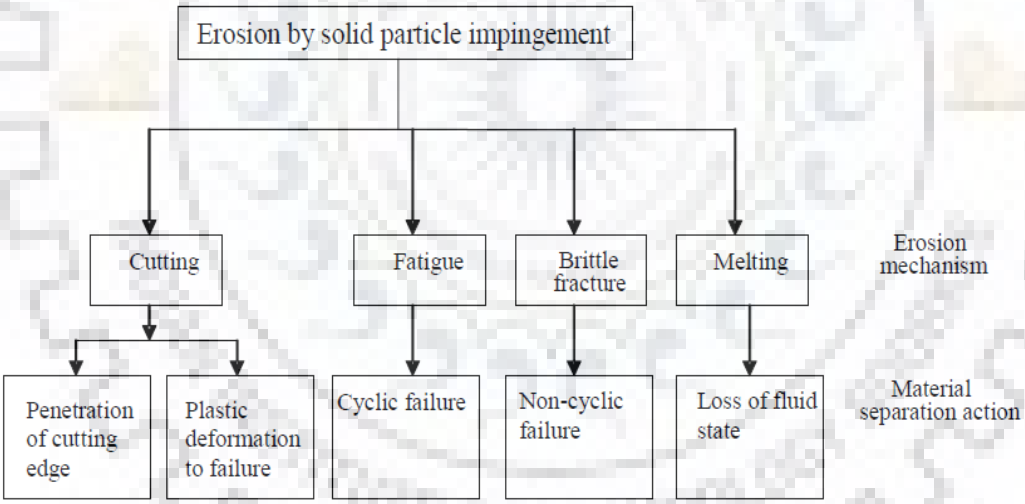

Figure 2.1: Hierarchy of Erosion Process [16].

Stachowiak and Batchelor [17] discussed seven different possible mechanisms for solid particle erosion such as abrasive erosion, surface fatigue, brittle fracture, ductile deformation, surface melting, macroscopic erosion and atomic erosion. Among all solid particle erosion, only first four (abrasive erosion, fatigue, plastic deformation and brittle fracture) are applicable to erosion of hydraulic machinery.

2.2.1 Mechanism of Abrasive wear and Erosive wear

As shown in Figure 2.2, the erosion mechanism is called abrasive erosion when sediment particles strike the surface of the material at low impingement angle and remove the material by cutting. When they touch surface, the abrasive grits roll or fold and cause abrasion or cutting mechanism to erode.

Due to surface fatigue on rolling surfaces, the surface fatigue erosion mechanism is comparable to wear. The surface can not be plastically deformed when the particles hit the s urface at big impact angle but at low velocity as shown in Figure 2.2. Instead, owing to fatigue action, the surface becomes fragile and cracks are launched after repeated punching in the surface. After several strikes, the particles will be separated from the ground. The plastic deformation of the surface results from the formation of the flakes around the striking stage when the particles hit the elastic surface with a medium velocity and a big angle of impression. The material will be detached as debris with repeated strike on the flakes. When particles strike the fragile surface at medium velocity with a big angle of impingement, erosion occurs through fragile fracture. If the particles are sharp, then there is a greater chance of brittle fragmentation and the particles break away from the fabric by cracking the surface.

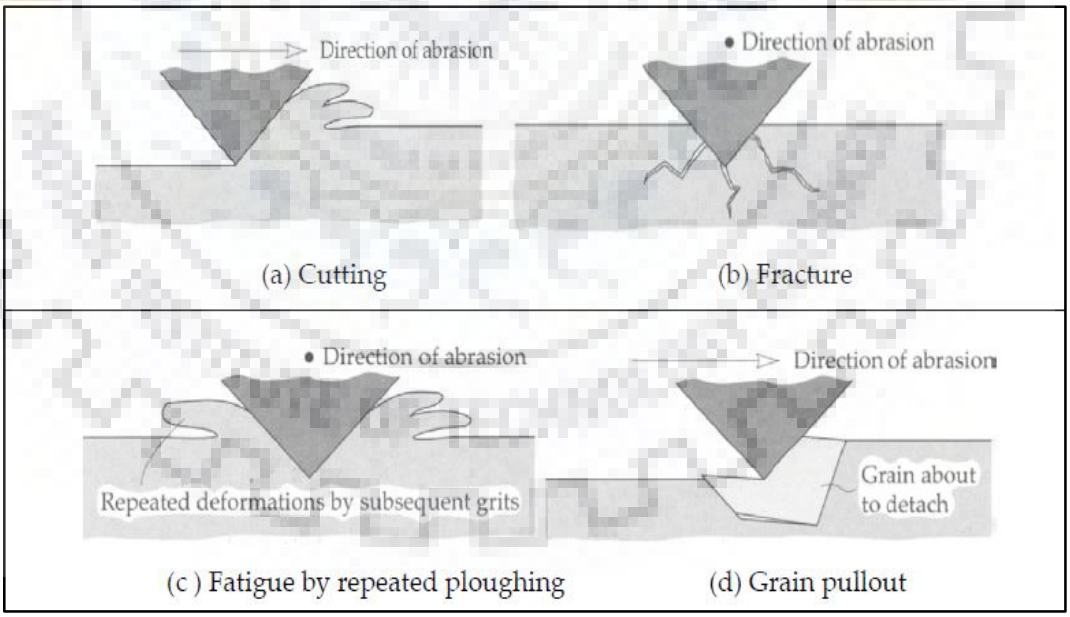

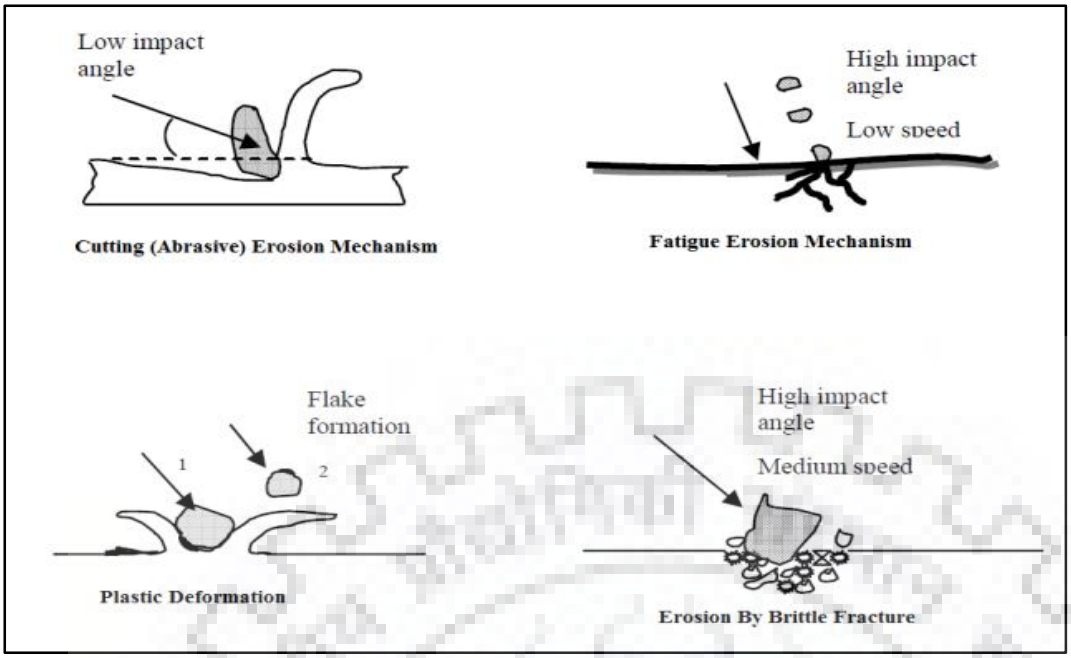

Figure 2.2: Mechanisms of Abrasive wear and Erosive wear [17].

2.3 FACTORS RESPONSIBLE FOR SAND EROSION

The various factors affecting the sand erosion are classified in three points as follows

I. **Operating conditions** -Velocity, acceleration, impingement angle, flux rate or concentration, medium of flow, temperature
II. **Eroding particles (sand or liquid droplets)** - Particle size, shape, hardness, material.
III. **Substrates (target materials)** - chemistry, elastic property, hardness, surface Morphology.

Among all other factors, velocity, angle of impingement and concentration of particles are most important and applicable to all forms of components where erosion takes place. These terms also appear in practically all erosion models. The angle of impingement is defined as the angle of the particle just before the effect between the eroded surface and the trajectory. If the particles move parallel to the surface, the angle of impingement is nearly 0° and therefore only minor erosion can occur. The impingement angle is 90° when particles move normally to the surface. Ductile and brittle material exhibits distinct erosion behavior patterns against angles of impingement. Figure 2.3 shows the variation in the erosion rate for ductile and brittle material against the impingement angle. This curve is widely adopted for maximum erosion of ductile and brittle materials [17].

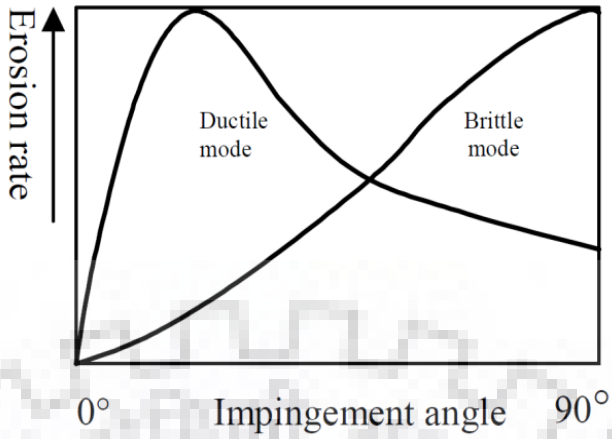

Figure 2.3: Schematic illustration of the erosion rate as a function of the impingement angle for brittle and ductile material [17].

Stachowiak and Batchelor [17] showed erosion rate (about 10 % of the maximum) even at zero-degree impingement, which could be due to the manner to describe the actual particle impingement angle. The jet angle is normally considered for practical purposes as an impingement angle of particles, but this is not the real angle of impact. Particle flow may be considered to have impingement angle zero in the straight pipe or parallel plates, but even in such flow erosion can be predicted. In such circumstances, if the flow is turbulent, the particles within the boundary layer could be dancing or oscillating in the normal direction of the flow, and hence the effective impingement could even be approximately 90°. The particle's impact velocity has a very dominant wear rate effect. Often there is a threshold speed below which wear is negligibly low. The relationship between wear rate and effect velocity is described by a power law and is given in Equation 2.1 for medium to high speeds covering most practical problems.

$$\frac{-dm}{dt} = kv^n \qquad (2.1)$$

Where,

m is the mass of the worn or damaged specimen (negative, since wear involves mass loss) kg

t is the duration of the process (s)

k is an empirical constant;

v is the impact velocity [m/s]

n is a velocity exponent.

The exponent ‘n’ value is generally in the range of 2 to 3 for solid particles which is slightly above any prediction based on kinetic energy of the particle. The equation is not comprehensive even though the value of ‘k’ is controlled by other parameters such as particle

density and shape for which there are no analytical data available. It is one of the early equations used to show the effects of velocity on wear rate, e.g. as particle velocity increases 10 times the wear rate can increase between 100-1000 times. Mostly erosion rate is considered as linearly proportional to concentration.

Bjordal [18] observed that erosion rate $\propto$ (concentration)^n where n varies from0.25 to 1.27 for distinct metals and coatings. But for the most of materials, if tested for longer periods of time, this value is close to 1. Therefore, considering the erosion rate direct proportional to concentration with regard to velocity is a satisfactory approximation. Fluids such as air, water, hydraulic oil and lubricating oil convey the erosive particles. The conveying medium features have a powerful impact on the erosion rate. The following variables or characteristics of the conveying medium influence the final rate of erosion

- **Bulk properties of fluid:** Density, viscosity.
- **Nature of flow:** Laminar or turbulent.
- **Microscopic properties:** Corrosively, lubrication, cooling effect.

The viscous fluid imposes drag force on the eroding particles and affects the rate of erosion by changing the impingement angle is described by Hojo et al. [19]. The particle trajectory and viscosity impact on the angle of impingement is shown in Figure 2.4. The impact of the erosive medium is evaluated in terms of "collision efficiency," which is a proportion of particles that in the presence of eroding medium effectively hit the eroding surface to the theoretical amount of particles that hit the eroding surface in the absence of the medium. The trajectory of particles is influenced by the flow medium. Comprehensive analysis of the particle trajectory can determine the accurate rate of erosion. Examples of the effect of particles rebounding from prior blades or buckets are erosion on the back side of the Pelton turbine bucket and gas turbine blade. If the direction of flow is parallel to the surface, but the flow is turbulent, the material erosion rate is higher than that of the laminar flow. More particles are likely to come into contact with the surface in turbulent flow and the same particle can hit the surface repeatedly. The particles will try to follow the streamline in laminar flow and may escape without hitting the surface, thus reducing the rate of erosion. The opposite will be the case if the fluid flow is directed to the surface normally, i.e. Erosion rate will be higher. Figure 2.5 shows the picture of particle behavior in laminar and turbulent flow. Small lubricant introduced to the liquid medium offers cooling during particle impingement, restricting changes in material characteristics and thus considerably reducing the erosion rate [19].

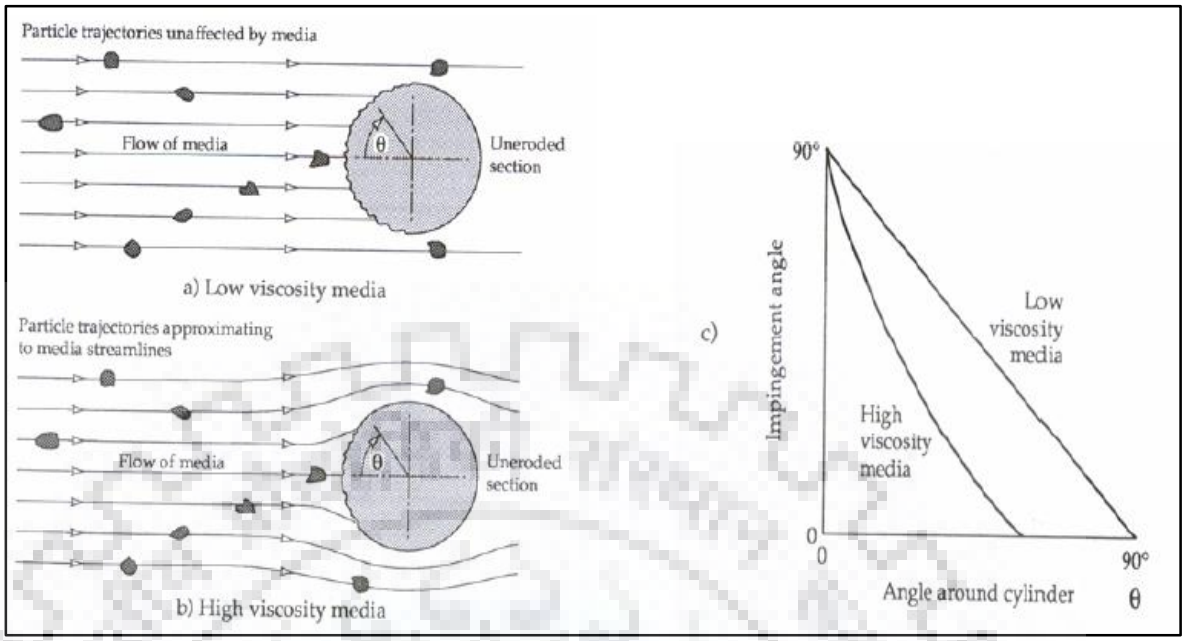

Figure 2.4: Medium effect on angle of impingement [19].

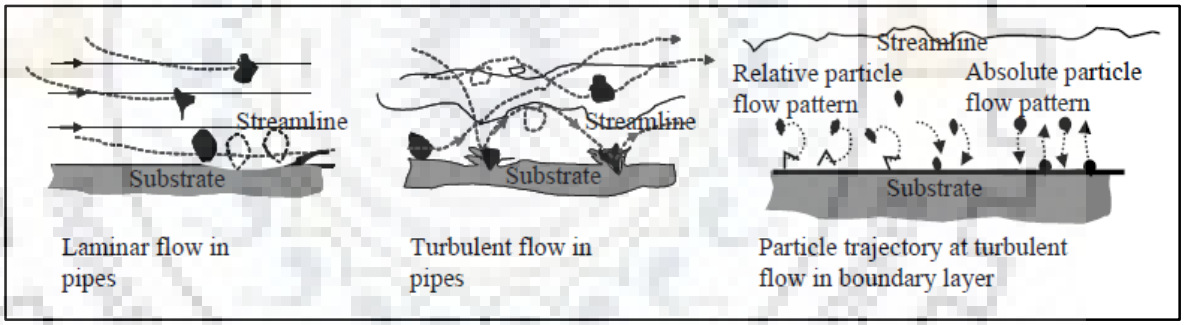

Figure 2.5: Effect of fluid flow conditions on particles of erosion [19].

Rai and Kumar[20] suggested different techniques for measuring suspended sediment parameters such as particle size measured in terms of median grain size (d_{50}).d_{50} refers to the average graded particle size not exceeding 50% of particle mass. The different instruments used to measure suspended parameters relevant to hydro-abrasive erosion are shown in Figure 2.6

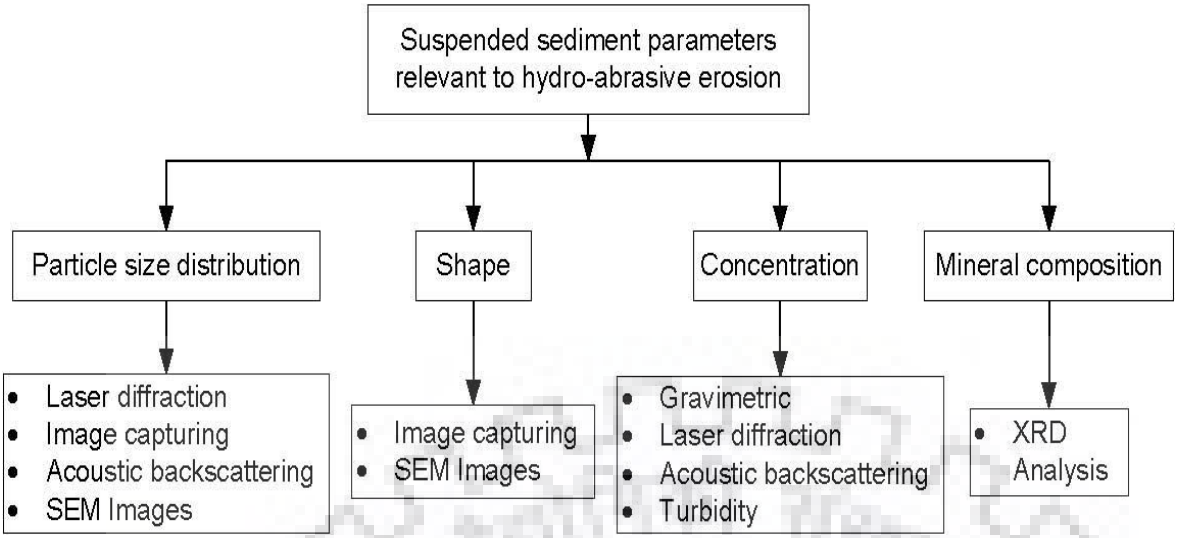

Figure 2.6 Parameters of suspended sediment related to hydro-abrasive erosion [20].

Particle size can be defined primarily by mass and length in two fundamental dimensions. For a given velocity, particle kinetic energy is proportional to mass, and spherical particle mass is equal to (diameter) ^{3}. Thus, in theory, the rate of erosion is equal to (diameter) ^{3}. Sheldon and Finnie [21] noted the change from ductile erosion mode to brittle mode when particle size changes from smaller to bigger. Maximum erosion rate shifted from impact angle 30° to 80° in the experiment with small and larger particles. Particles of small size have a more cutting impact, while larger particles deform material through elastic deformation and fatigue. In addition to the shift, there was a dramatic change in erosion rate and erosion resistance ranking as shown in Figure 2.7 along with the change in erosion mode. In the occurrence of erosion due to small particles, the erosion rate ranking depends on hardness, whereas in the case of large particles it depends on material toughness. The particle size not only harms the wearing rate but also drastically changes the wear resistance ranking of materials. The materials ranked according to their wear resistance are in the following order when the small particles were used as the erosive agent: high density aluminum > annealed aluminum > plate glass > high density magnesium > graphite and hardened steel. In this case, the erosive wear rate depends on the hardness of the material apart from the annealed aluminum. In this instance, work to harden the aluminum could be significant. On the other hand, when large particles were used as an erosive agent, the order changes to annealed aluminum > hard steel > high aluminum density > high magnesium density > glass plate > graphite. So the toughness of material is

important in this condition.

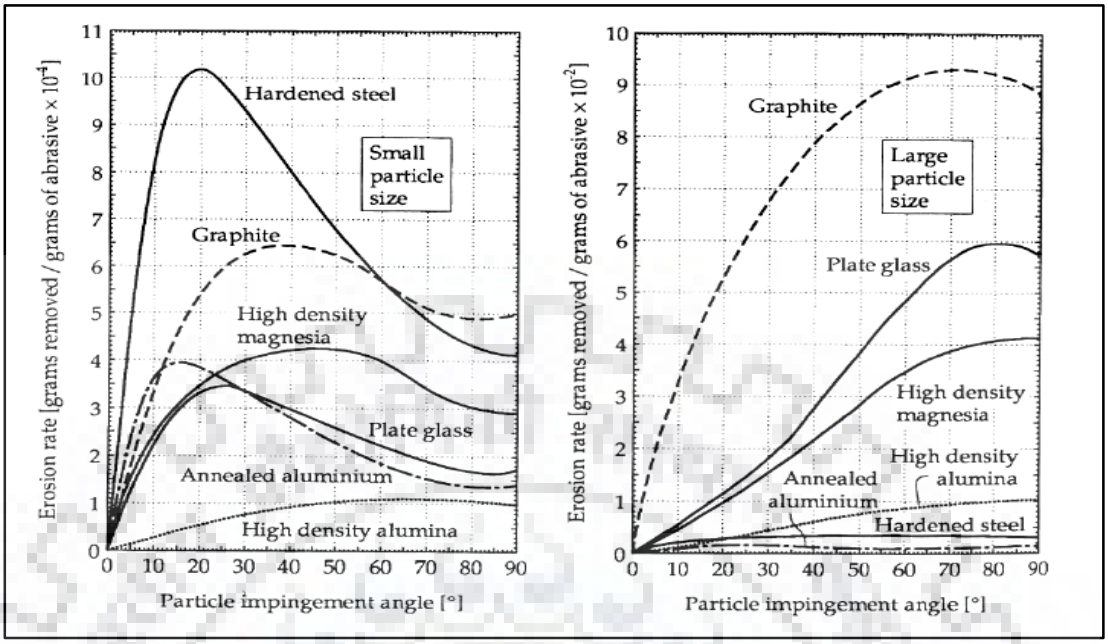

Figure 2.7: Ranking of erosion resistance based on Sheldon and Finnie silicon carbide erosion test at velocity of 152 m/s [21].

Bahadurand and Badruddin [22] discussed various approaches to characterization of particles; as shown in Figure 2.8. Some characterization parameters that are commonly used are:

i. Maximum length of separation 'L' along a line between two points.

ii. Maximum stability plane factor: length, width and thickness.

iii. The diameter of a circle equal to or equal to the projected perimeter dp.

iv. Sphere diameter of equal area ds or volume dv (also known as nominal diameter).

v. These ratios are unity for regular bodies (e.g. Sphere) = (L / W) and flakiness ratio = (W / T). The reciprocal of elongation ratio is called "Aspect Ratio."

In river hydraulics, non-cohesive natural sediments are most often characterized in terms of particle diameter. This process can be suitable for other sediments with comparable shape and density to natural sediments. Particle dimensions of sediments are explained in terms of sediment diameter, standard fall diameter, nominal or sieve diameter. The standard fall diameter of a particle is the diameter of a sphere that has a specific gravity of 2.65 and has the same terminal settling velocity as the given particle in 24° C calm distilled water.

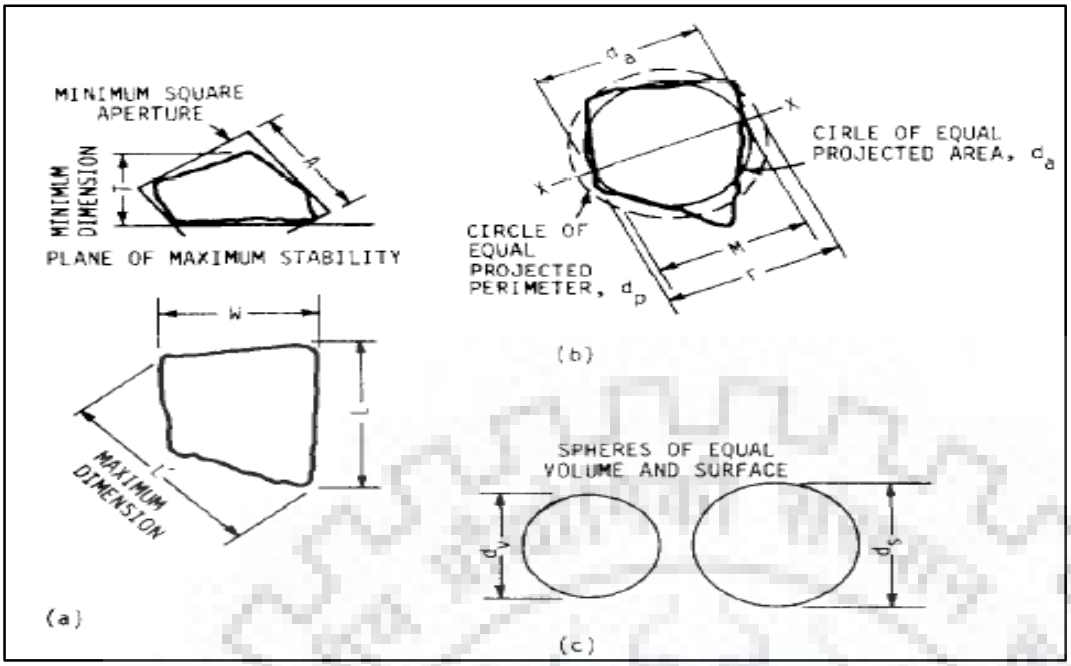

Figure2.8: Definition of particle shape [22].

The basic shapes found in nature are normally uniform, but the actual shapes of particles are sharp and complex due to several reasons, which cannot be defined in mathematical terms. The particle shape is a good indicator of the erosion process, for instance, irregular shape with sharp edge ncreases the rate of erosion, while blunt particles with round edges decrease that usually occurs. Most erosion models introduced the shape impact; therefore, quantification of the shape parameter is essential for the estimation of solid particle erosion. In addition to some of the methods proposed by Bahadur and Badruddin [22], roundness factor (Perimenter2/4 π Area) and other statistical parameters are used to describe the particle shape. Correlating the shape of particles can also be explained in terms of "Rake angle," which is the angle between the front face of the particle and normal to the target surface, when the ductile erosion is linked with cutting by a single point cutting tool.

Chen and Li [23] simulated erosion using computer model (Micro-scale dynamic model, MSDM) and investigated three basic shapes of the erosion rate difference; triangle, square and circle as shown in Figure 2.9. Triangular particle followed by circular and square is the highest erosion loss in the single particle impact. This observation is compatible with interaction area pressures. The loss of erosion changes when the square particle is rotated at 45 ° and the contact is shortened. In reality, several particles strike the surface and in this case the erosion ranking will be different as shown by 50 particles in impacts. In this case, erosion by square shape particle is bigger than circular,

because of plastic deformation after subsequent strikes is in larger area. Overall, triangular or rectangular particle erosion rates can be 1.5 times greater than rectangular particles. Wear rises quickly for metals in particular once the hardness of the particles exceeds that of metal for both scouring and abrasion of impact. Beyond this, with the increasing abrasive hardness, the wearing rate may become relatively constant, or even reduce. Particle shape and hardness complement one another. Even severe erosion may not occur with hard but relatively sharp particles. Hard particles tend to have a sharp appearance; by comparison, even with a small effect, the edges of soft particles round off. If the particles are harder than the substratum, there is severe erosion, but if the particles are softer, erosion occurs only if the substratum has low strength.

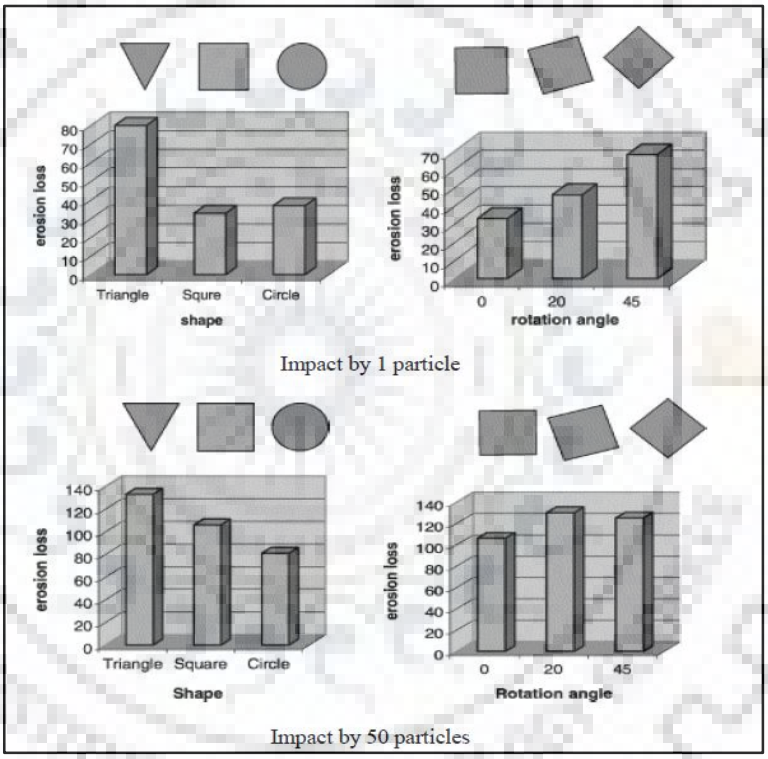

Figure 2.9: Erosion rate due to different shapes of particles [23].

In the relative Erosion rate due to different shapes of particles term of Moh's hardness scale 10 between 1 for talk powder as well as 10 for diamond, the mineral hardness is generally represented. Knife edge hardness in Moh's scale is 5.5 and steel needle hardness is 6.5. The sediments of the river are in the form of clay, silt, sand and gravel with specific gravity approximately 2.6. Sediment particles are classified in the river hydraulics into bed load and suspended load depending on sediment transport. All the particles that slide, roll or jump close to the bed are called as bed load. These particles are much lower in velocity than flowing water, whereas all those particles that are carried away in suspension by flowing

water are called suspended load and have almost the same speed as flowing water. The suspended load fraction is settled in the settling basins or reservoirs and the rest passes through turbines causing erosion of components. Due to chemical and mechanical weathering, sediments are made of rock fragmentation. The river sediments are mixtures of different particle sizes as shown in Table 2.1. It is basically a sand fraction of the sediment that causes the erosion of turbines. Further classification of the sand percentage can be made in fine (0.06-0.2 mm), medium (0.2-0.6 mm) and coarse (0.6-2 mm) [24].

Table 2.1: Classification of river sediment [24]

Particle	Clay	Silt	Sand	Gravel	Cobbles	Boulders
Size(mm)	<0.002	0.002-0.06	0.06-2	60-250	22-60	>250

Rai and Kumar [25] presented an overview of available techniques for assessing hydro-abrasive erosion and suspended sediments, helping investigators and hydropower engineers to measure and mitigate hydro-abrasive erosion.

Padhy and Saini [26] widely reviewed the silt erosion field. Different factors related to silt erosion in hydro turbines are discussed on the basis of literature surveys. Different reasons for declining hydro turbine performance and suitable remedial measures proposed by different investigators are also discussed. In their review, they studied that researchers reported that the improvement is not significant in most instances, despite design changes in the turbine components and providing different materials and coating to the turbine blades. After the literature review it was suggested that further experimental and theoretical studies are essential to study the effect of hydro-abrasive erosion.

Padhy and Saini [27] conducted an experimental study to investigate, under actual flow conditions, the erosion mechanism of a small-scale Pelton turbine bucket. Samples of silt were gathered from the Head work of one of the hydropower stations most affected by silt. Based on the investigation, silt size has been found to be a strong parameter for producing erosion, and the removal of material from the surface is due to plastic deformation and surface ploughing.

2.4 EROSION MODELS

Erosion designs are helpful for designing turbine parts, sediment settling basins, and optimizing hydropower plant operation in sand-laden waterways. Individual particle dynamics are most often used to develop models of erosion. Empirical and statistical relationships were also developed from experimental and field measurements. However, the number of erosion models in the hydraulic machineries are validated for their reliability.

Generally speaking, erosion harm is regarded as the gradual reduction of material caused by repeated deformation and cutting behavior. The real erosive wear mechanism was not fully

understood. A simple, effective and generalized quantitative model for erosion could therefore not be created.

Truscott [28] found that the most frequently quoted expression for erosion is

$$Erosion \propto (velocity)^m \quad (2.2)$$

Bardal [29] describes the most general formula for pure erosion

$$W = K_{mat}.\ K_{env}.\ C\ .f(\alpha)\ V_p^m\ \left[\frac{mm}{year}\right] \quad (2.3)$$

Where, W is erosion rate (material loss) in mm/year.

$K_{mat}.$ is material constant.

K_{env} is constant depending on environment.

C is concentration of particles.

$f\ (\alpha)$ is function of impingement angle α.

V_p is the velocity of the particle.

m is the exponent of velocity.

Tsuguo [30] developed a relationship of factors contributing to turbine erosion based on erosion data from 18 hydropower plants.

$$W = \beta.\, C^x.\, a^y.\, k_1.\, k_2.\, k_3.\, V^m \left[\frac{mm}{year}\right] \quad (2.4)$$

Where

W is loss of thickness per unit time

β is turbine coefficient of eroded part

V is relative flow velocity.

The term a is average grain size coefficient on the basis of unit value for grain size 0.05 mm.

The terms k_1 and k_2 are shape and hardness coefficient of sand particles.

k_3 is abrasion resistant coefficient of material.

The$x$, y are exponent values for concentration and size coefficient respectively.

Padhy [31] has developed a correlation to estimate percentage efficiency loss of rated efficiency for Pelton runner as shown in Equation (2.5).

$$\eta\% = 2.43 \times 10^{-10}(t)^{.75} \times (S_p)^{0.099} \times (C)^{0.93} \times V^{3.4} \quad (2.5)$$

Where

$\eta\%$ is percentage efficiency loss of rated efficiency in operating hours (t),

S_p is silt particle size in mm.

C is silt concentration (ppm).

V is velocity of flow (m/s).

Bajracharya et al. [32] established spear erosive wear and efficiency reduction relationships

from the field survey of Chilmi Hydro Electric Plant (CHEP), a Pelton turbine-based hydroelectric plant in Nepal. They introduced a relationship between the erosion rate and the particle size at different quartz content which is described as

$$E_r \propto a(size)^b \left[\frac{mm}{year}\right] \quad (2.6)$$

E_r is the erosion rate, a and b are empirical constants

a = 351.35, b=1.4976 for quartz content of 38%

a = 1199.8, b=1.8025 for quartz content of 60%

a = 1482.1, b=1.8125 for quartz content of 80%

$$\eta_r \propto a.(E_r)^b \quad (2.7)$$

η_r is loss in runner efficiency per year due to erosion alone a= 0.1522 and b= 1.6946

It was found that the erosion rate of 3.4 mm/year for the needle and bucket results in efficiency reduction of 1.21 percent thereby causing loss of power generation.

A technical committee of IEC formulated a concept for the modeling of hydro-abrasive erosion on hydraulic turbines for applied engineering purposes. This concept and general design recommendations have been published in the IEC guideline 62364 (2013) [9, 33].It gives a factorized equation for the absolute erosion rate, considering the following parameters:

$$\frac{\Delta de}{\Delta t} = \frac{k_f}{RS^P} k_m w^x SSC k_{size} k_{shape} k_{hardness} \left[\frac{mm}{hr}\right] \quad (2.8)$$

Where

Δt Exposure period[h].

Δde Depth of erosion during Δt [mm].

K_f Coefficient reflecting the flow pattern, i.e. angle of attack and turbulence intensity, a constant for each turbine component.

RS Reference size of a turbine [m]; for Pelton turbines *RS* = inner bucket width B.

P Exponent, a constant for each turbine component, for consideration of curvature -dependent effects.

K_m Coefficient for the material at the surface of a turbine part, K_m = 1 for martensitic stainless steel with 13% Cr and 4% Ni; K_m < 1 for coating material.

w Characteristic relative velocity between the flow (or the particles) and the turbine part [m/s].

x Exponent, IEC suggests the value as 3.4, literature values range

between 2 and 4.

SSC Suspended sediment mass concentration [g/l] = [kg/m^3], for Pelton SSC = 0 if no flow.

K_{size} Coefficient for particle size, IEC suggests to take the numerical value of d50 in [mm], d_{50} is the median size of graded particles which is not exceeded by 50% of the particle mass.

K_{shape} Coefficient for particle shape, IEC suggests the value of $k$shape = 1 for rounded, 1.5 for sub angular and 2 for angular particles.

$K_{hardness}$ Coefficient for particle hardness with respect to the hardness of the surface of material, IEC suggest to take the mass fraction of particles harder than the surface material.

Rai [34] implemented the IEC-62364 erosion model on Toss HPP, a 10MW Small Hydro power Plant located in Himachal Pradesh and observed values of unknown coefficients such as flow coefficient (K_f) and reference size exponent (p) for different regions of Pelton bucket significantly damaged by erosion. The values are given in Table 2.2.

Table 2.2: Values of unknown coefficients of IEC-62364 erosion model [34].

Unknown co-efficient of IEC-62364 erosion model	**Components of Pelton bucket**	**Values obtained**
Flow factor (k_f)	Splitter height reduction	1.76 x 10^{-5}
	Erosion in cut-out region	2.99 x 10^{-5}
	Erosion depth in bucket outlet	5.43 x 10^{-6}
Exponent of reference size (p)	Splitter height reduction	0.1458
	Erosion in cut-out region	-0.038
	Erosion depth in bucket outlet	0.2959

He also worked on the average value of material factor (Km) for 13 Cr- 4Ni WC-Co-Cr HVOF coating in his research work and the result obtained is 0.12 with 17.82 as coefficient of variations.

Padhy and Saini [35] conducted an experimental study and had developed a correlation for normalized erosive wear rate as shown in Equation (2.9).

$$w = 4.02 \times 10^{-12} \times (S) \times (C) \times (V)^{3.79} \times (t) \quad (2.9)$$

Where

W is erosive wear rate,

S is silt size,

C is silt concentration,

V is water jet velocity and

t is the operating hour of the turbine.

Thapa [36] performed laboratory experiments of several turbine components to determine erosion rates under different experimental conditions. His findings suggest the following empirical relation to predict the erosion rate for 16Cr5Ni, which is the most widely used turbine material.

$$y = 6E - 5x^{3.13}\ [mg/kg] \quad (2.10)$$

Where $x\ m/s$ is the velocity of eroding particles impinging at the angle of 45˚ and y is loss of the material in $mg\ /\ kg$ of eroding particles striking the surface.

Krause and Grein [37] recorded the abrasion rate on conventional steel Pelton runner made of X5CrNi 13/4 and the abrasion rate estimate equation is given in Equation (2.11).

$$\delta = pqcv^{3.4}\, f(dp_{50}) \quad (2.11)$$

Where δ is abrasion rate (μm/h), p is a constant, q is quartz content, c is mean silt concentration, v is relative velocity, $f\,(dp_{50})$ is function defining particle size. This equation holds good for turbine made up of X_5CrNi 13/4 material.

Table 2.3 Summary of literature review carried out under this study.

S. No.	Authors	Remarks
Theoretical investigations		
1.	Thapa et al. [15]	(i) The hydro-abrasive erosion is a complex phenomenon depending on many various factors which can be broadly divided in three groups (a) operating conditions, i.e. velocity, acceleration, impingement angle, type of fluid, temperature; (b) erodent particles properties (sediment parameters), i.e. Particle concentration, Particle shape, Particle size, Mineral hardness, mineral composition; and (c)substrate (target material) properties, i.e. elasticity, hardness, surface0morphology
2.	Bhushan [16]	(i) Recognised six principal wear mechanisms, which have distinct phenomenons. (ii) He defined that wear is removal of solid material from rubbing surfaces.
3.	Stachowiak and Batchelor [17]	(i) Discussed abrasive erosion, surface fatigue, brittle fracture, ductile deformation, surface melting, macroscopic erosion and atomic erosion as seven different possible mechanisms for solid particle erosion. (ii) Found that abrasive erosion, fatigue, plastic deformation and brittle fracture are applicable for hydraulic machines.

4.	Bjordal [18]	(i) Found erosion rate $\propto$ (concentration) ^{n} where n varies from 0.25 to 1.27 for distinct metals and coatings. But for most materials, if tested for longer periods of time, this value is close to 1. (ii) He came up with an approximation that erosion rate is directly proportional of concentration with respect to velocity.
5.	Hojo et al. [19]	(i) Discussed the trajectory of particles and effect of viscosity on impingement angle. (ii) Showed the effect off fluid flow conditions on erosion particle.
6.	Rai and Kumar [20]	(i) Suggested different techniques for measuring suspended sediment parameters.
7.	Sheldon and Finnie [21]	(i) Noted the change from ductile erosion mode to brittle mode when particle size changes from small to bigger. Maximum erosion rate shifted from impact angle 30° to 80° in the experiment with small and larger particles. (ii)The erosion rate ranking depends on hardness in case of erosion due to small particles, whereas in case of large particles, it is dependent on toughness of material.
8.	Bahadurand and Badrudin [22]	(i) Discussed various approaches of particle characterization. (ii) Suggested roundness factor as one of the factors to describe the shape of the particles.
9.	Chen and Li [23]	(i) Simulated erosion using computer model (Micro-scale dynamic model, MSDM) and the difference in the erosion rate in three basic shapes; triangle, square and circle (ii)The highest erosion loss in single particle impact is by triangular particle followed by circular and square. This observation is in agreement with stresses induced by the contact area.
10.	Lysne et al. [24]	(i) Classified the river sediments into clay, silt, sand, gravels, cobbles and boulders on the basis of particle size (mm).

11.	Rai and Kumar [25]	(i) Presented an overview of available techniques for assessing hydro-abrasive erosion and suspended sediments, helping investigators and hydropower engineers to measure and mitigate hydro-abrasive erosion
12.	Padhy and Saini [26]	(i) Reviewed the field of silt erosion widely. (ii) Suggested that further experimental and theoretical studies are essential to study the effect of hydro-abrasive erosion.
13.	Padhy and Saini [27]	(i) Conducted an experimental study to investigate, under actual flow conditions, the erosion mechanism of a small-scale Pelton turbine bucket. (ii) Found that silt size is a strong parameter to produce erosion in turbines.
Erosion models		
14.	Truscott [28]	(i) Found the most frequently quoted expression for erosion.
15.	Bardal [29]	(i) Describe the most general formula for pure erosion.
16.	Tsuguo [30]	(i) Developed a relationship of factors contributing to turbine erosion based on erosion data from 18 hydropower plants.
17.	Padhy and Saini [31]	(i) Developed a correlation to estimate percentage efficiency loss of rated efficiency for Pelton runner.
18.	Bajracharya et al. [32]	(i) Established spear erosive wear and efficiency reduction relationships from the field survey of Chilmi Hydro Electric Plant (CHEP), a Pelton turbine-based hydroelectric plant in Nepal.
19.	IEC-62364 (2013) [33]	(i) Formulated a concept for the modelling of hydro-abrasive erosion on hydraulic turbines for applied engineering purposes. (ii) Developed a factorized equation for the absolute erosion, considering different parameters.
20.	Padhy and Saini [35]	(i) Conducted an experimental study and had developed a correlation for normalized erosive wear rate.
21.	Thappa [36]	(i) Performed laboratory experiments of several turbine components to determine erosion rates under different experimental conditions.

22.	Krause and Grein[37]	(i) Recorded the abrasion rate on conventional steel Pelton runner made of X5CrNi 13/4.

2.5 GAPS IDENTIFIED

An extensive literature review have been carried on sand erosion of turbines particularly for Pelton turbine to identify and understand the various parameters in which study has to be carried out and an attempt has been made to find out the scope for future work in the field of sand erosion of Pelton turbine. Based on literature review the following gaps have been identified.

i. To relate the sediment properties with the hydro-abrasive erosion, suspended sediment concentration (SSC) and total suspended sediment load (SSL) are widely used but these parameters do not consider particle size, shape and mineral composition into account for erosion.

ii. The flow condition created in the test rigs do not represent the actual flow conditions as in the turbine. Therefore, a study is required to create the actual flow conditions as in the turbine in order to accurately predict the erosive wear of turbines in practice.

iii. The various correlations and models studied in the literature review show that some parameters of erosion models are dependent on site conditions. Hence, a study is required to validate the erosion model based on site conditions for further accurate results.

2.6 OBJECTIVE OF THE STUDY

It is proposed to carry out field study to investigate the effect of sand erosion on Pelton turbines installed at Chenani Hydroelectric power plant with the following objectives.

i. To study the various components of Chenani hydroelectric project-I, (CHEP-I).

ii. To collect the sediment samples and conduct sediment measurements using various techniques and instruments.

iii. To analyze the measured sediment parameters such as concentration , size, shape and mineral content and hardness and to estimate erosion rate and efficiency reduction using available erosion models in Pelton turbine installed at ROR based Chenani hydroelectric project-I.

2.7 PROPOSED METHODOLOGY OF THE PRESENT WORK

Based on the above discussed specified points, the various steps which are followed in the methodology, are listed below. A flow chart reporting the methodology is shown in Figure 2.10.

i. **Study of various components of chenani Hydroelectric power plant, (CHEP-I).**

The detail study of various components of CHEP-I like civil works, electromechanical and hydro mechanical have been done during the site visit.

ii. **Collection of suspended sediment sample**

The dry as well as suspended sediment samples of sand have been collected from the study site through visiting site.

iii. **Analyzing suspended sediments parameters**

The different sediment parameters have been measured and analyzed with the laboratory based equipment like LISST, SEM, and XRD etc. to get the values of these parameters which are required to investigate their effects on the turbine.

iv. **Erosion models and Correlations for estimating erosion rate and efficiency changes**

Erosion models like IEC-62364 and available correlations as discussed in literature are selected to estimate erosion rate and efficiency reduction of Pelton turbine installed at CHEP-I. The results obtained from the various erosion models are discussed for the chenani hydroelectric project-I.

v. **Conclusion**

Based on results and discussions, conclusions are drawn and for future studies recommendation are made.

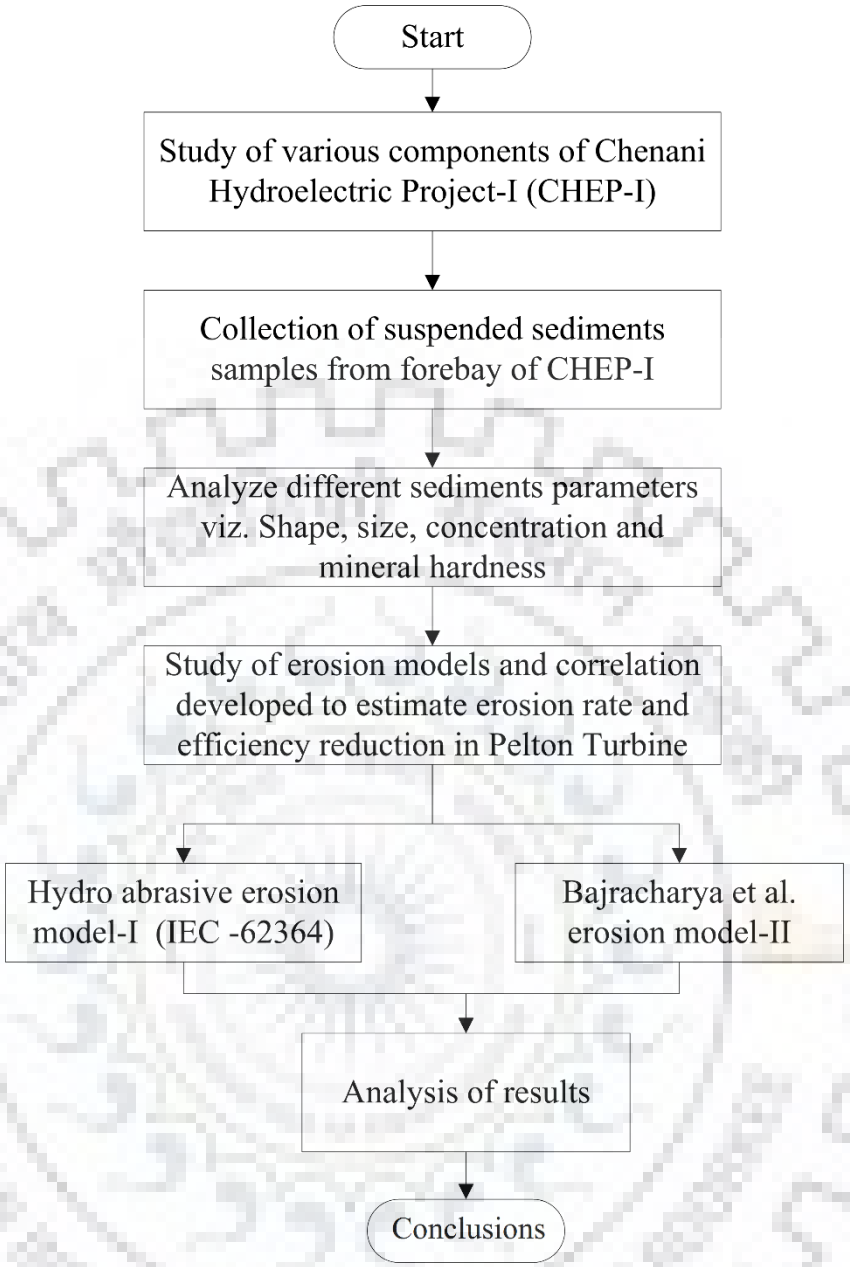

Figure 2.10: Flow chart showing methodology adopted for the present study

CHAPTER 3
DETAILS OF CHENANI HYDRO ELECTRIC PROJECT-I

3.1 GENERAL

As discussed earlier under Chapter 2, the objective of the present study is to collect the sediment samples and analyze sediment parameters to investigate the erosion rate and efficiency reduction of Pelton turbine, Accordingly Chenani Hydro Electric Project-I has been considered under this study. This Chapter presents the details of the CHEP-I.

3.2 CHENANI HYDROELECTRIC PROJECT- I

The state of Jammu and Kashmir is located in northern India. The state region lies mostly in the Himalayan Mountains and shares its borders in its south with other countries such as Himachal Pradesh and Punjab. There are three areas in Jammu and Kashmir: Jammu, Kashmir and Ladakh. Jammu and Kashmir state is one of the potential regions for generation of Hydro power as the important river basins of State having a significant potential of power generations which includes Indus and its tributaries, Jhelum and its tributaries, Chenab and its tributaries; as well as Tawi river[39].

The Eastern Tawi River is one of the primary tributaries of the Chenab River, which originates from Lahus in the hilly region northwest of Bhaderwah in Jammu Province. Tawi, Ujh and Nira streams, Chenab tributaries have their source in Kailash Lake. Tawi initially takes the southern path for a distance of 40.2 km and then follows the northwestern path up to Chenani. Of the complete catchment of 2167.80 km^2, only 209.70 km^2 is supplied by snow. The river catchment area along with the river path from the origin up to Jammu with respect to the fall is used for the hydropower generation. Since CHEP-I is fed by the river run, with only one pick-up weir, the actual silt content of the stream does not affect the proposition as there is no storage engaged. Due to its steep path and consequent elevated speed during floods, Tawi River rolls down large rocks during the rainy season. During minor floods, it holds fine and medium silt. Sturdy trash rack are fixed at the intake of the canal to reduce the introduction of rocks and silt into the water conductor. A settling tank is also built near diversion weir to reduce the silt content in water power channel. The water sample containing silt has revealed harmful quartzite particles of a size of 1.33 mm × 2 mm and above remains in the flow during the rainy season [40].The problem of sand erosion is also observed in CHEP-I as the Tawi River carries a lot of sediment along with water into the water conductor. During monsoon, the concentration of the particle increases and quartz content is also very high, which erodes

the profile of the component and thus reducing the efficiency of the turbine.

The Chenani Hydroelectric Project-I is fed from East Tawi, one of the main tributaries of the Chenab River that flows from Lake Kailash in the hilly region southwest of Bhaderwah in Jammu Province, as its actual source. The CHEP-I has installed capacity of 23.30MW and its head works is located at Benisang 6 km upstream of Chenani town and has 18.34 km length of water conductor system comprising of various components i.e. tunnels, open channel and wooden flumes. At the tail end of the water conductor system there is a big forebay tank having temporary storage capacity of 17.42 lacs cft. (50000 cum). This run-of-river SHP has design discharge of 8.5 m^3/s and net head of 365 meters and is equipped with 05 units of twin jet Pelton turbines each of having rated power of 4.66MW.The two penstocks having a length of about 1 km have been provided from forebay tank to power house and have been bifurcated to 5 units near turbines. Figure 3.1 shows the view of Chenani Hydro Electric Project-I and a Google view of Chenani Hydro Electric Project-I shown in Figure 3.2.

Figure 3.1: View of Chenani Hydroelectric project-I

Figure 3.2: Google view of Chenani Hydroelectric Project- I located in district Udhampur of J&K.

3.2.1 SALIENT FEATURES OF CHENANI HYDRO ELECTRIC PROJECT-I

LOCATION

State	Jammu and Kashmir
Province	Jammu
District	Udhampur
Year of commissioning	6th September 1971-unit No. I, II& III 24th May 1975-unit No. IV 21st August 1975-unit No. V

HYDROLOGICAL DATA

S. No.	Particulars	Location/Parameter
1	Name of the river.	Weir site about 6 kms
2	Head works	Upstream of chenani town
3	Power House	Laddan
4	Length of canal	18.64 kms
5	Minimum discharge of river water	1.27 cumecs
6	Maximum discharge	3936 cumecs at head flood
7	Normal discharge during Summer	15.52 cumecs
8	Slope	1 in 98
A	**HEAD WORKS AT BENISANG**	
1	Weir Type.	Rock fill Weir
2	Length of weir.	225 ft. across the river between Flanks
3	Bed level of weir	1069.89 m
4	Crest level (spill way)	1070 m.
5	Maximum H.F. level crest.	1075.944 m
6	Maximum H.P. level before construction	1071.37 m

B	**GATES**	
1	Size of gates	03 No's (4.57 m x 3.04 m)
2	Clear width of gates	4.57
3	Clear depth of gates	3.04 m
4	Maximum discharge through head gates	200 cusecs
5	Bed level of head regulator in front of gates	1069.23
6	Crest level of head gate	1069.23
7	Top level of head gate	1072.28
8	Highest floods level of river	1075.94
9	Bed level of canal of H/W	1066.419
C	**COVERED CHANNEL**	
1	Length	3.36 kms
2	Bed width	7 ft.
3	Height of covered channel	8.250 ft. upper section
4	F.S.L	1.955 m
5	Bed grade	1 in 1000
6	Maximum discharge	5.66cum
C	**TUNNEL**	
1	Length(horse shoe type)	9.90 kms (3 Nos.)
D	**FOREBAY**	
1	Length of tank	213.36100 m (average)
2	Bed width	30.48 m (average)
3	Full supply depth	5.48m
4	Hill side slopes	1:1.25
5	Downstream slopes	1.1.25
6	Capacity	4.93 crore litres
7	Bed width of canal trench	2.74
8	Side slope	Vertical

9	F.S.L	1.143m

E PENTOCKS

		I	II
1	Length of Penstocks	1034.18 m	1046.68 m
2	Discharge	5.09 cumecs	3.39 cumecs
3	Diameter	1.52 m to 1.21 m.	1.21m to 0.9144 m

The general layout of Chenani hydro electric project-I is shown in Figure 3.3.

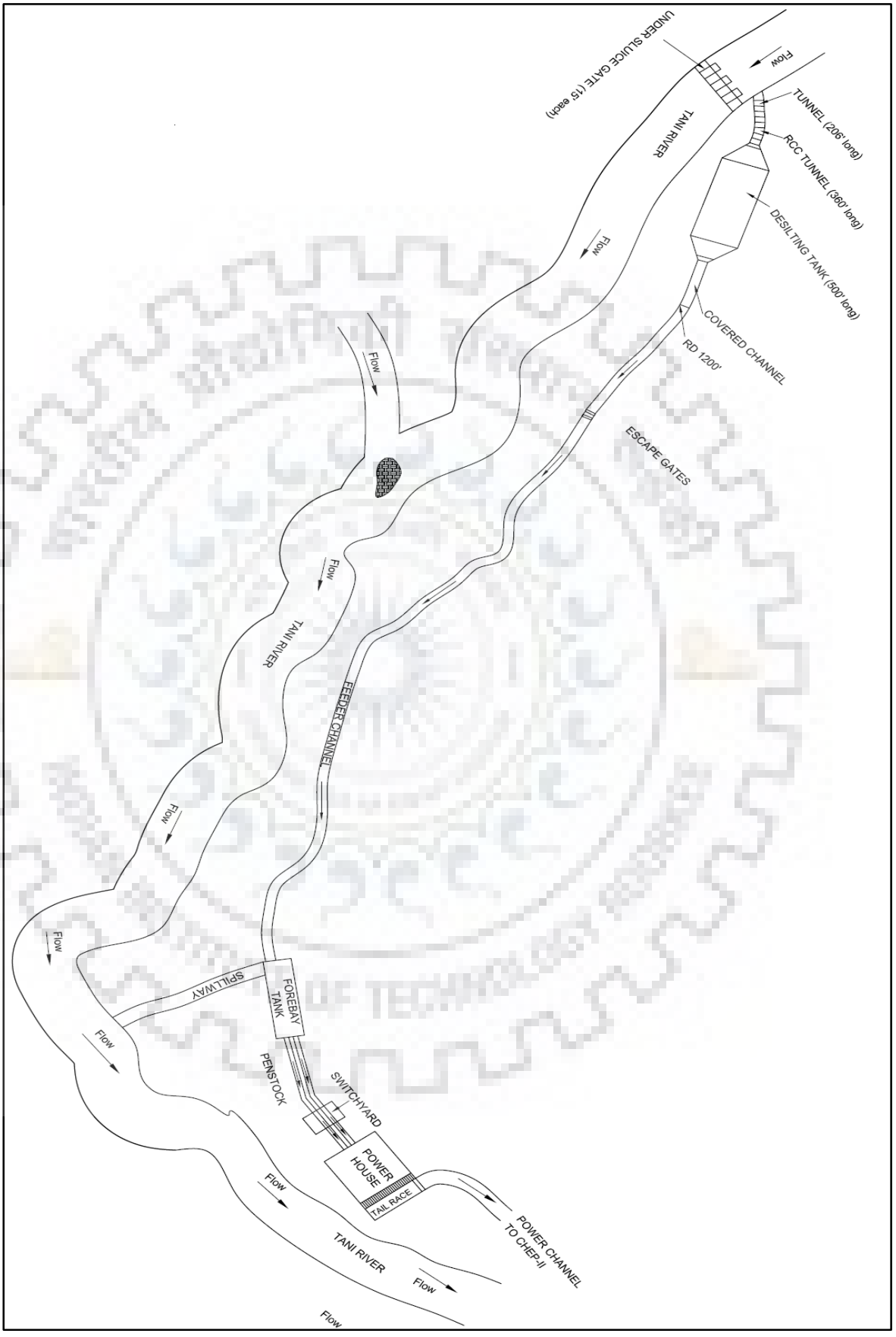

Figure 3.3: General Layout of Chenani hydroelectric project-I.

3.3.1 Civil components

The hydropower power plant is divided into three categories as; Civil works, Electrical equipments and Hydro mechanical components. The civil components of hydropower plant comprises of diversion weir, desilting tank, power channel or water conductor, forebay, power house building and tail race channel.

3.3.1.1 Diversion Weir

It is located about 6 km upstream of the Tawi River from Chenani town. It is conventional type pickup weir as shown in Figure 3.4, perpendicular to river axis having 4.57 m × 3.04 m under sluice gates. It diverts water to the left side of the flow of river. Figure 3.5 shows the photographs of diversion weir of Chenani hydroelectric project-I

Figure 3.4: Google image of Diversion weir.

Figure 3.5: Diversion weir of CHEP-I.

3.3.1.2 Desilting tank

A desilting tank is provided to settle the particle size up to 0.25mm. The dimensions of the settling tank is 11m × 15.24 m × 2.5 m with tapering ends on both sides. It is aligned parallel with power channel. An escape gate is also provided at one side near the outlet of the settling tank to flush out the silt which resides in the tank as shown in Figure 3.6.

Figure 3.6: Desilting Tank

3.3.1.3 Power Channel

The power channel of this project is trapezoidal in shape and about 18.34 km in length with different type of profiles. Channel is mostly made of concrete but at some places it is in the form of wooden flumes and tunnels. There are wooden flumes at two different locations which act as good water carrier in sinking zones where concrete channel may damage due to erosion of soil bed under the power channel. The wooden planks act as a single unit over large span of area and do not damage due to erosion hence carry water efficiently in sinking zone. Figure 3.7 shows the photograph of trapezoidal power channel and the part of power channel made up of wooden flumes is shown in Figure 3.8.

Figure 3.7: Trapezoidal Power channel of CHEP-I.

Figure 3.8: Wooden flumes channel of CHEP-I.

3.3.1.4 Forebay tank

It is large temporary storage tank of 4.93 crore liter capacity having maximum water depth of 5.5 m. The average length and breadth of forebay is 230 m × 30.48 m. The discharge is taken through two penstocks to turbines. The minimum draw down level of the penstock is about 2.7 m. It has concrete bed on its all sides with fencing mounted on it. It is easily accessible by road. The trash cleaning of the trash racks installed at Penstock intake are cleaned regularly as to maintain the pressure of the penstocks at the downstream side. Figure 3.9 shows the photograph of Forebay tank taken from upstream side

Figure 3.9: View of the Forebay tank taken from upstream side.

3.3.1.5 Penstock

There are two penstocks avaliable of dimeters (1.52 m to1.21 m) and (1.2 m to 0.91 m) as shown in the Figures 3.10 and Figure 3.11 respectively.The length of penstocks is 1034 meters and is mainly exposed and buried near the powerhouse. The one penstock is trifurcated and feeding and the other one is bifurcated and feeding discharge to last two generating units. Material used in manufacturing of penstocks is mild steel.These penstocks are laid on 127 R.C.C saddles and also 11 anchors are provided along the length.

Figure 3.10: Layout of Penstocks of CHEP-I.

Figure 3.11: View of Penstocks taken from downstream side.

3.3.1.6 Power house building

It is two storeyed building of 54 m × 16.7 m dimensions consisting of machine hall, control room (22.2 m × 10 m) on the north, underground hall, and workshops, office and staff room. It adjusts all the five generating units and other mechanical and electrical components. The Capacity of each generating unit is 4.66 MW. Figure 3.12 shows a google view of Power house and Figure 3.13 shows the machine hall of CHEP-I.

Figure 3.12: Google view of Powerhouse of CHEP-I.

Figure 3.13: Machine hall of CHEP-I.

3.3.1.7 Tailrace channel

This is a rectangular shaped R.C.C channel (65.5 m × 3.65 m × 2.43 m) that conducts water from the power house to power channel of CHEP-II. Designed capacity of this tail race is 8.49 cumecs. It has escape gate at its back side through which water can be rejected directly to river when CHEP-II is under maintenance. Figure 3.14 shows the photograph of Tailrace channel of CHEP-I.

Figure 3.14: Tailrace Channel.

3.4.2 Electromechanical component - Pelton turbine

The five Turbine - Generator units at CHEP-I are horizontally placed and have identical design. Each turbine of Pelton type has two nozzles and one runner with design discharge of 1.52 m^3/s each, a rated power of 4660 kW and runs at 600 RPM under net head of 365.76 m. The specific speed of the each turbine is 25.606.The diameter of jet d_o is 21 mm for design discharge. The jet deflectors are provided for all nozzles. All the parts of the turbine except runner are uncoated and made of steel with lower erosion resistance compared to runner. The runners have a pitched circle diameter D_1 =1212m, an outer dia. of 1540m and a mass of 1219 kg. Each runner has 21 buckets with an inner width B at 334mm. i.e. D_1/B is 3.63 The fully casted runner has a weight of 1219 kg and made up of 1.4317G - X_4CrNi 13-4 material. These runners were manufactured by M/S Andritz Hydro in the year 2012 and high velocity oxy fuel coating (HVOF) have been applied over them. The nozzle seat ring and spear are not hard

coated. The twin jet horizontal Pelton turbine installed at CHEP-I is shown in Figure 3.15.

Figure 3.15: Twin jet horizontal shaft Pelton Turbine installed at CHEP-I.

CHAPTER 4
MEASUREMENT OF SEDIMENT PARAMETERS

4.1 GENERAL

As discussed earlier, The CHEP-I is facing the problem of sand erosion since its inception but no investigation of erosion due to sand have been carried out. To study the effect of sand erosion on Pelton turbine, CHEP-I is selected. The forebay is selected to collect the homogeneous suspended sediment samples for measurement of sediment properties such as concentration, particle shape, size and mineral hardness on a regular basis during study period as shown in Figure 4.1. The suspended sediment samples of Chenani Hydroelectric Project-I were collected near intake of Penstock, the point where the particle content is going through the turbine. Manual homogeneous samples were collected on a daily basis from June 2017 to 13 September 2017 in 1 litre of plastic bottle as per the water sampling procedure mentioned in IEC 62364 (2013) [9].The sediment analysis of abrasive particles in the water going through the turbine include all the suspended sediment parameters which are necessary to evaluate the hydro-abrasive erosion action the particle can have on the turbine parts.

Figure 4.1: Collection of suspended sediment samples from Forebay of CHEP-I during study period.

The suspended sediments are characterized by the parameters like particle size distribution, particle concentration, shape and mineral hardness. These suspended sediments samples are brought to HRED, Environment laboratory to analyze the sediment properties and then the numerical value of these sediment properties are used to find out the erosion rate and efficiency reduction in the turbine by using various erosion models and correlation developed so far. The

working principle of instruments, their range of measurement and accuracy are discussed in detail in this chapter. These details of the instrument are given in Table 4.1

Table 4.1: Details of the instrument used in the study

S. No.	Properties measured	Name of Instrument	Working Principle of instrument	Range of measurement	Resolution and accuracy	Remarks
1	Median Particle size (d_{50}) and volumetric concentration.	LISST-Portable (sequoia)	Laser diffraction	SSC: 0.1-100mg/l (depends on PSD) PSD: 32 sizes from 1.25µm-250µm	SSC: <1µl and ± 15%	Manual samples from CHEP-I
2	Particle shape	FE-SEM (carl Zeiss)	SEM (Scanning Electron Microscope)	-----	Up to 0.6mm	Sediment samples from CHEP-I
3	Total suspended sediments (TSS)	HA 0.45µm (Millipore) BT 224 S (Sartorius)	Filter Paper	Residue from 100 ml sample taken	0.45µm	Manual sediment samples from CHEP-I
4	Mass of Filter paper	BT 224S (Sartorious)	Electromagnetic force restoration	0-220g	1 mg	Manual sample for gravimetric analysis.
5	Turbidity	2100P Portable Turbidimeter (Hach)	Optics	0-1000 NTU	0.01 NTU and ±2 % of reading plus stray light	Manual sediment samples from CHEP-I

4.2 SUSPENDED SEDIMENT PARAMETERS

The sediment properties like size, shape, concentration and mineral hardness are measured, analyzed and numerical values are obtained to find erosion rate and efficiency changes in turbine using erosion models and correlations developed under previous studies and available in literature.

4.2.1 Particle size distribution (PSD)

The Knowledge of particle size gradient making up the sediment load is a basic

requirement for understanding the sediment's source, transport, and environmental impact. The particle size in a river varies from clay to cobble. Suspended load rarely contain anything larger than coarse sand. In the present study, the classification of sediment particles by size (diameter), according to DIN EN ISO 16488-1 is used and is shown in Figure 4.2. The boundary between sand and silt (63 μm) separates coarse grain sediments (sand and larger particles) from fine grain sediments (layers of silt and mud). Coarse grain sediments are non-cohesive while fine grain sediments are cohesive. As different particle sizes have different behaviour in the flow of water, this has an impact of their type of damage on the turbine parts. IEC-62364 (2013) recommends the measurement of median particle size to calculate the Particle load (PL) passing through the turbine over specified time

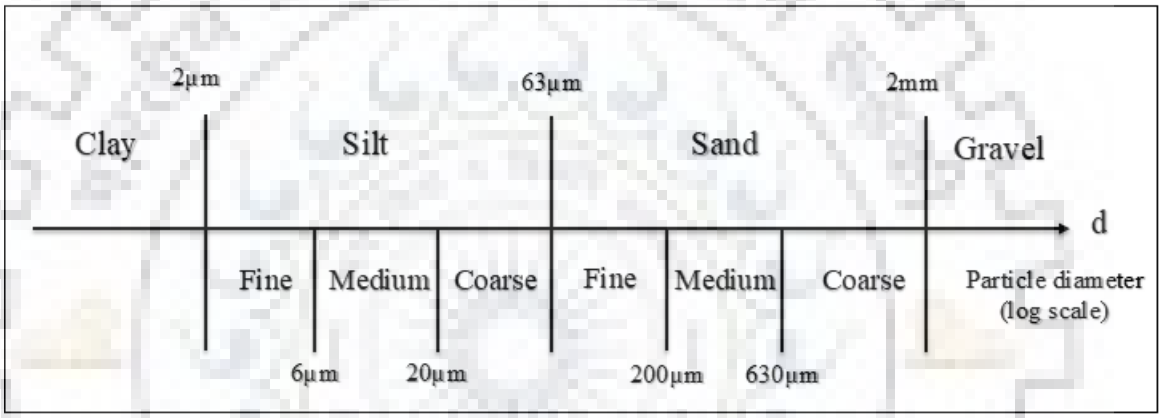

Figure 4.2: Classification of Sediment particles [30].

There are different methods of measuring particle size like Sieve analysis, SEM images etc. The portable laser diffraction instruments have become available under the trademark – LISST stands for 'Laser In-situ scattering and transmissometry' and gives the value median grain size (d_{50}) of the particle and volume concentration accurately. The manual collected samples are brought to the laboratory. LISST portable (sequoia) is a particle size analyzer which is used to determine different grain sizes and volume concentration of sediment sample. The value of median grain size (d_{50}) is used to estimate erosion rate by using erosion models. This Scattered laser light is received by a multi-element photo detector composed of series of ring-shaped progressive diameter sensors that enable the estimation of the beam dispersion angle as shown in Figure 4.3. Particle size can be calculated by knowing the value of this angle using the fraunhoffer approximation.

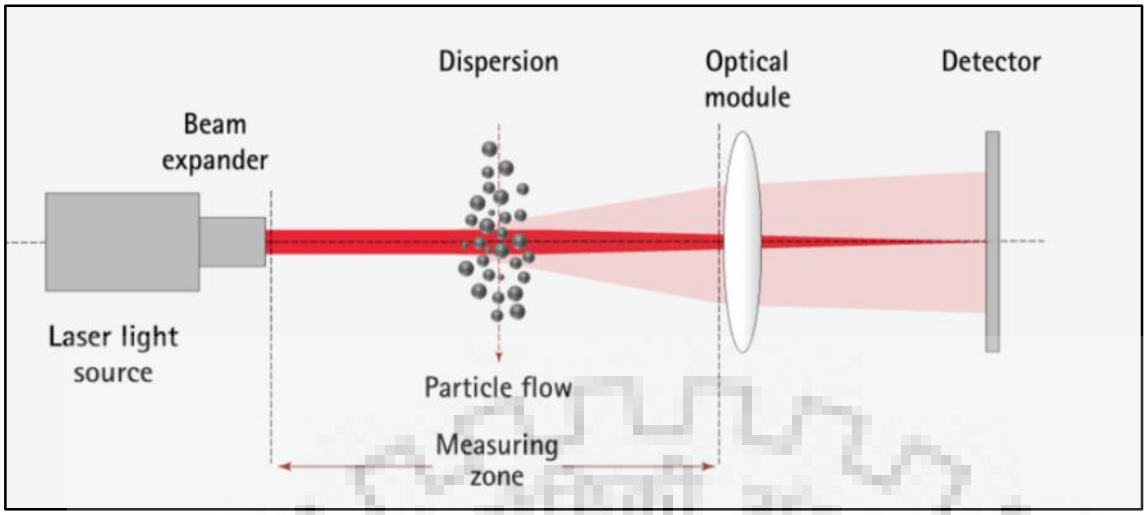

Figure 4.3: Principle of Laser diffraction [38].

The working principle of working of instrument is discussed in the above and the steps involved in analyzing particle size using LISST portable is provided in the following manner. The photograph of the instrument is shown in the Figure 4.4.

Figure 4.4: Image of LISST -Portable (sequoia)

The various steps involved in analyzing the value of different grain sizes during the operations of LISST equipment are arranged in sequence. Firstly, switch ON the instrument by pressing the button provided on the top right side. The main menu appears on the screen. To begin with measurement process, touch the measure icon as shown in Figure 4.5. The measurement process is divided into several steps as discussed below.

Figure 4.5: Main menu screen of LISST- Portable particle size analyzer

I. Rinse chamber

The first step as shown in Figure 4.6 is to rinse the mixing chamber with clean water multiple times. Make sure that there is no residual of previous sample left in the mixing chamber. Switch ON the mixer button. Fill the sample chamber with distilled or deionized water.

Figure 4.6: Image of Rinse chamber screen of LISST- Portable particle size analyzer

II. Get background

Press update button to measure the clean water background. Make sure mixer runs at a constant speed during the process. Rinse the chamber twice after completing the reading. (Figure 4.7).

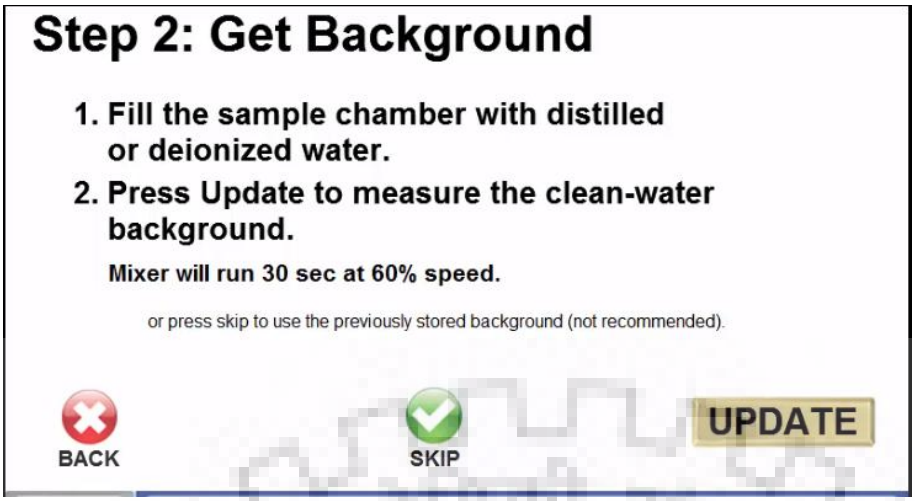

Figure 4.7: Image of background screen of LISST- Portable particle size analyzer

III. Add sample

Add sample to the mixing chamber. Pour sample slowly to mixing chamber to minimize bubbles. Fill the chamber completely before starting the mixer**.** (Figure 4.8).

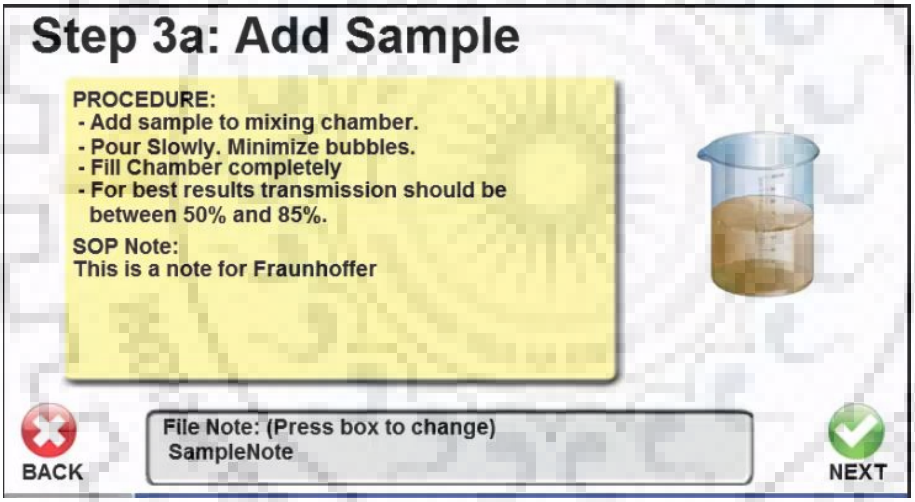

Figure 4.8: Image of add sample screen of LISST- Portable particle size analyzer

IV. Preparing sample

The sample is prepared automatically using ultrasonic and mixing settings. The blue pointer should be in green zone to get accurate results**.** Too many particles or too fewer particles may cause inaccurate results. (Figure 4.9).

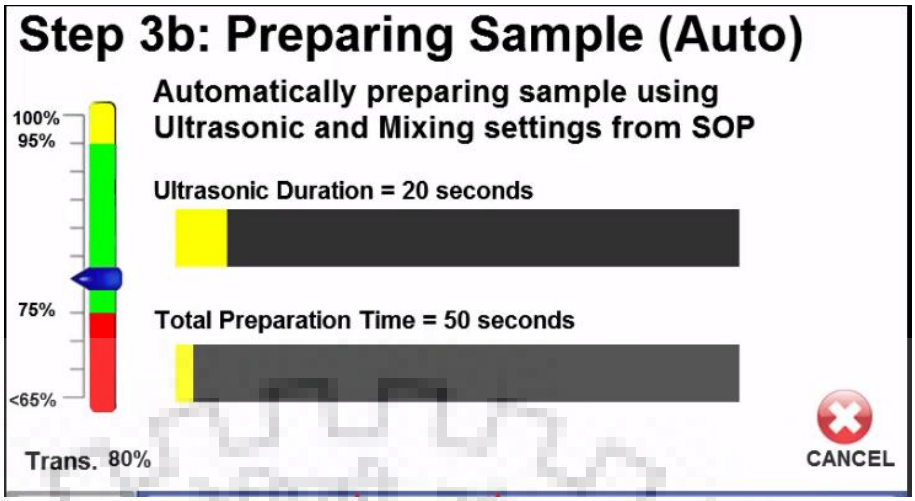

Figure 4.9: Image of preparing sample screen of LISST- Portable particle size analyzer

V. Acquire average

During the acquired average, the light scattered by the particles is recorded over the duration. The light scattered is then used to compute the size distribution. (Figure 4.10).

12

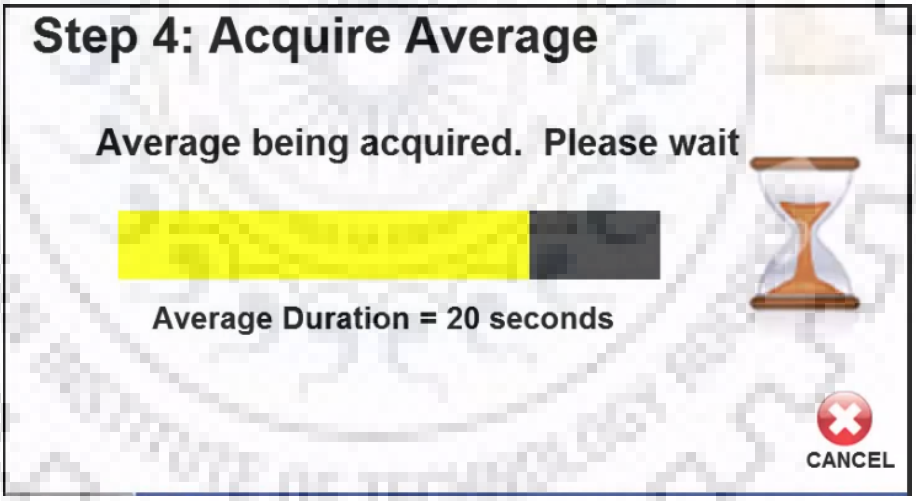

Figure 4.10: Image of acquire average screen of LISST- Portable particle size analyzer

VI. Compute size distribution

It takes around 10 seconds to compute size duration. The chamber may be drained and rinsed while the size distribution is computed**.** (Figure 4.11).

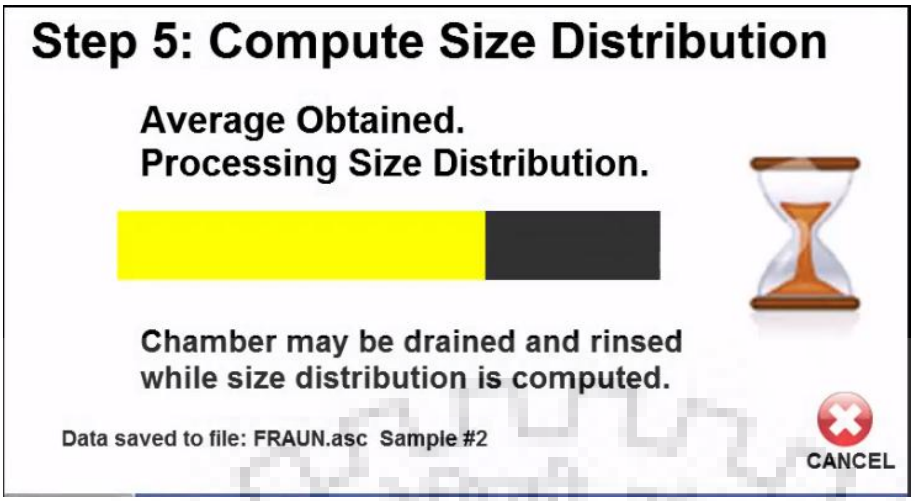

Figure 4.11: Image of size distribution screen of LISST- Portable particle size analyzer

VII. Sample report

The sediment sample data is stored in the instrument and can be retrieved from the data logger of the instrument by connecting it with computer. The files are processed to fetch the sample data report. The size distribution report is shown in the Figure 4.12.

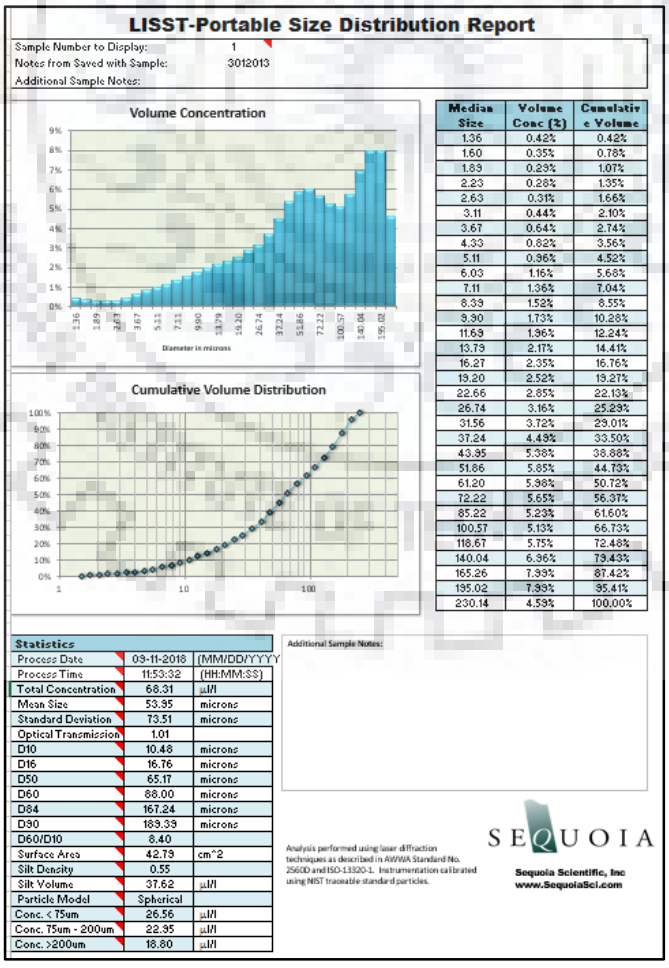

Median Size	Volume Conc (%)	Cumulative Volume
1.36	0.42%	0.42%
1.60	0.35%	0.78%
1.89	0.23%	1.07%
2.23	0.28%	1.35%
2.63	0.31%	1.66%
3.11	0.44%	2.10%
3.67	0.64%	2.74%
4.33	0.82%	3.56%
5.11	0.96%	4.52%
6.03	1.16%	5.68%
7.11	1.36%	7.04%
8.39	1.52%	8.55%
9.90	1.73%	10.28%
11.69	1.96%	12.24%
13.79	2.17%	14.41%
16.27	2.35%	16.76%
19.20	2.52%	19.27%
22.66	2.85%	22.13%
26.74	3.16%	25.29%
31.56	3.72%	29.01%
37.24	4.49%	33.50%
43.95	5.38%	38.88%
51.86	5.85%	44.73%
61.20	5.98%	50.72%
72.22	5.65%	56.37%
85.22	5.23%	61.60%
100.57	5.13%	66.73%
118.67	5.75%	72.48%
140.04	6.96%	79.43%
165.26	7.99%	87.42%
195.02	7.99%	95.41%
230.14	4.59%	100.00%

Figure 4.12: Image of particle size distribution report of LISST- Portable

4.2.2 Suspended sediment concentration

It is measured in terms of mass sediment concentration as well as volume concentration. It is non dissolved particles in the water which is measured in mg/l or in parts per million (PPM). The suspended sediment mass concentration is defined as ratio between mass of solid particles and the corresponding volume of water particle mixture. SSC does not include the concentration of dissolved minerals. The sediment concentration greatly varies in space and time (seasonally, diurnally, event based). SSC ranges from a few ppm (in the lean season) to thousands of ppm (during monsoon season or during flash floods). The mass level of suspended sediment concentration is generally determined in the laboratory using filtration technique to determine total suspended solids (TSS). In the present study, the same method is used to determine TSS.

The homogenous manually collected suspended sediment samples have been brought to laboratory from the site in cleaned plastic bottles and analyzed for suspended sediment concentration by using Filter Method. A total of 101 samples, each of having 100 ml has been filtered and a whatman filter paper of diameter 125 mm with a pore size 0.45μm is used and shown in Figure 4.13. The initial weight of filter paper is weighed on electronic weigh machine as shown in Figure 4.14 is recorded on the data sheet. A date is marked on the filter paper. Measure 100 ml of suspended sediment sample and pour the same through the funnel on which filter paper is placed. The experimental set up is shown in Figure 4.15. After pouring sample, wet filter paper is taken out from funnel and kept it for drying in an oven for 8 hours. These dried filter papers are removed and weighed again as shown in Figure 4.16. TSS has been calculated using Equation (4.13).

$$TSS = \left(\frac{W_{F+TSS} - W_F}{100} \right) \times 10^6 \qquad (4.13)$$

Where TSS is Total suspended sediments in mg / l (equivalent to ppm). W_{F+TSS} is filter paper weight with TSS, and W_F is the initial filter paper weight.

Figure 4.13. Specifications of Whatman filter paper

Figure 4.14: Initial weight of Filter paper measured with weigh machine (BT 224S Sartorius)

Figure 4.15: Experimental set up for performing gravimetric analysis

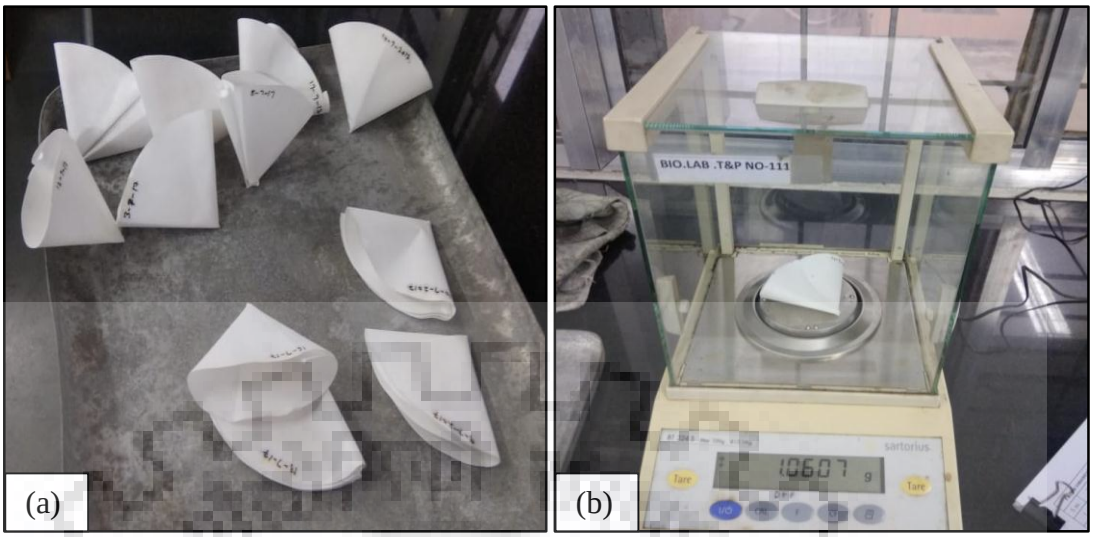

Figure 4.16: (a) Dried filter paper taken out from oven (b) Measurement of dried filter paper

The steps taken like folding of filter paper and placing it on the funnel and pouring the sample while carrying out garvimetric analysis of sediment samples are shown in Figure 4.17.

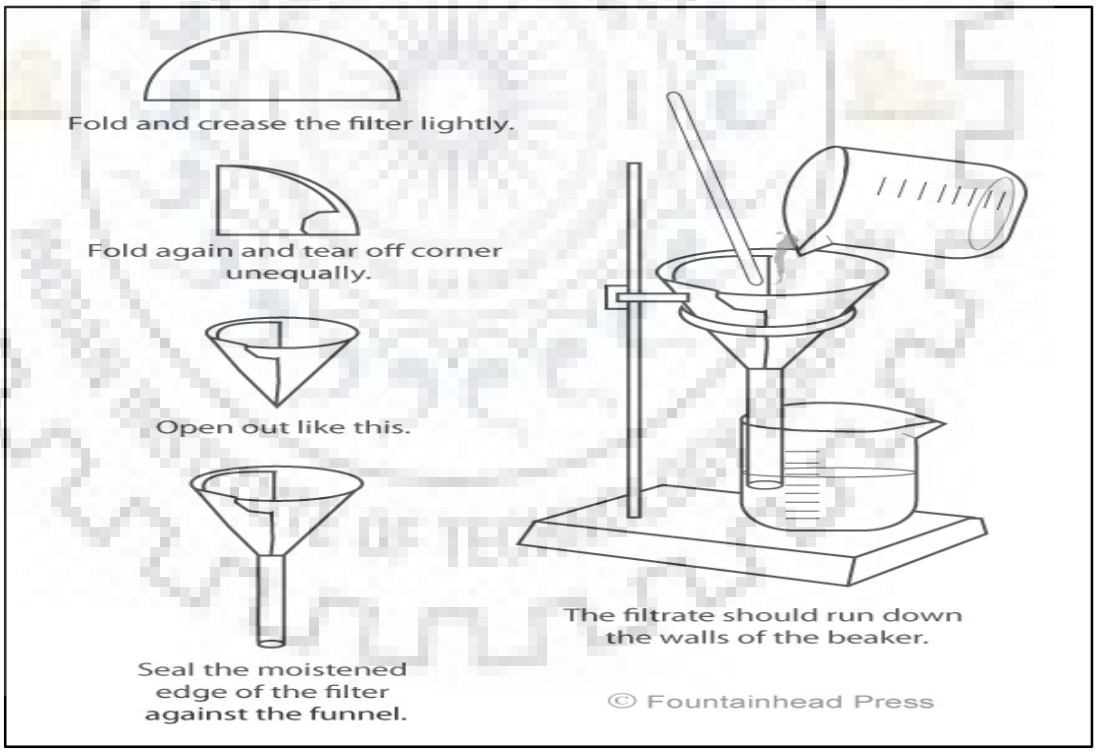

Figure 4.17: Procedure of performing gravimetric analysis

The volumetric concentration of suspended sediments is determined in the laboratory by using LISST Portable equipment. It is measured in micro litre per litre (µl/l).The mean size of the particle is also determined. The turbidity of manually collected homogeneous suspended

sediment sample is also measured using Portable Turbidimeter (Hach) 2100P which works on the principle of optics. It is measured in NTU. The photograph of the turbiditimeter is provided in the Figure 4.18.

Figure 4.18: Portable Turbidimeter 2100P (Hach)

4.2.3 Sediment shape

The quantification of sediment shape was carried out in multiple ways in literature such as shape, flatness, sphericity, elongation, and roundness. All parameters can be categorized primarily into two categories: (1) an aspect of the sediment particle spatial scale such as shape, sphericity and elongation, and (2) particle details in detail such as roundness. SEM (Scanning electron microscope) images under different magnifications as suggested in IEC-62364 (2013) were taken to visualize the form of typical particles and to see if either round particles or particles with sharp edges mainly present in the sediment. The Photographs of Scanning electron microscope (SEM) available in Institute instrumentation centre, IIT Roorkee and preparation of dried sediment sample to analyze sediment shape under SEM is shown in Figure 4.19 and 4.20 respectively.

Figure 4.19: Photograph of Scanning electron microscope

Figure 4.20: Preparation of sample

4.2.4 Mineral content and hardness

The mineralogical content of suspended sediment specimens is identified in the laboratory using X-ray diffraction analysis and quantified with petrography assessment as the effect on erosion varies significantly owing to distinct mineral hardness. A lot of petrography is done with a petrographic microscope - using a diamond saw and polisher, and then examine it under a special microscope in both normal and polarized light.The Moh's scale, a non- linear scale introduced in 1812, which is commonly used for sediment mineral hardness. XRF is a non-destructive analytical technique for determining the elemental structure of materials. It operates by emitting an X-ray photon beam that incidents on the sample atoms. The interaction of the main X-ray beam with the atoms of the sample excites the electron from the atoms of the sample and some electrons are knocked out of their positions and then this causes a vacuum. This is the reason why the atom is temporarily unstable. This movement causes energy loss and the quantity of this energy loss is relevant to each element. We can therefore analyze the amount of each component present in the sample. The Moh's hardness scale comes under resistance to scratching category and the hardness increases from 1 to 10, Talc (1) being the softest and Diamond (10) being the hardest and other minerals like quartz, Feldspar, mica which fall in between are used to standardize the scale by assigning a number to them. It is qualitative approach which is generally used by mineralogists to identify mineral hardness.

4.3 RESULTS OF SEDIMENT PARAMETERS

The results obtained from the measurement of sediment parameters are presented in the form of graphs. These results are discussed in details as follows.

4.3.1 Particle size

The different grain sizes of suspended sediments were measured and analyzed in the field using a mobile laser diffraction device LISST (Sequoia) with a measuring range of 1.25 – 250 μm. The PSD defines the particles of different sizes present in a sediment-water sample from a river. d_x denotes the diameter of particle which is not exceeded by x % of the particle mass [9]. The different values of grain sizes are shown in Figure 4.21.

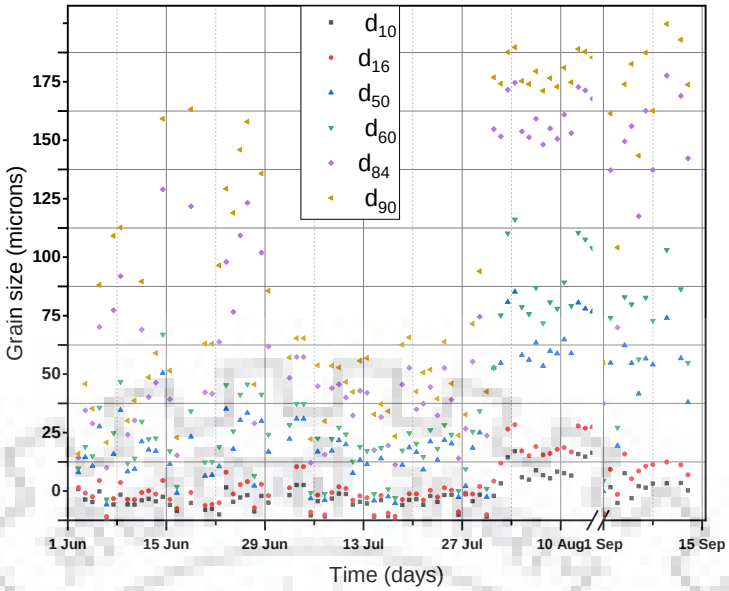

Figure 4.21: Particle size distribution of suspended sediments

The median grain size (d_{50}) obtained as a result of LISST portable based analysis from the manual collected sample are shown in Figure 4.22. IEC -62364[8] recommends the median grain size to be used for the calculation of particle load. The Particle load is used to estimate erosion depth of Pelton buckets using IEC erosion model.

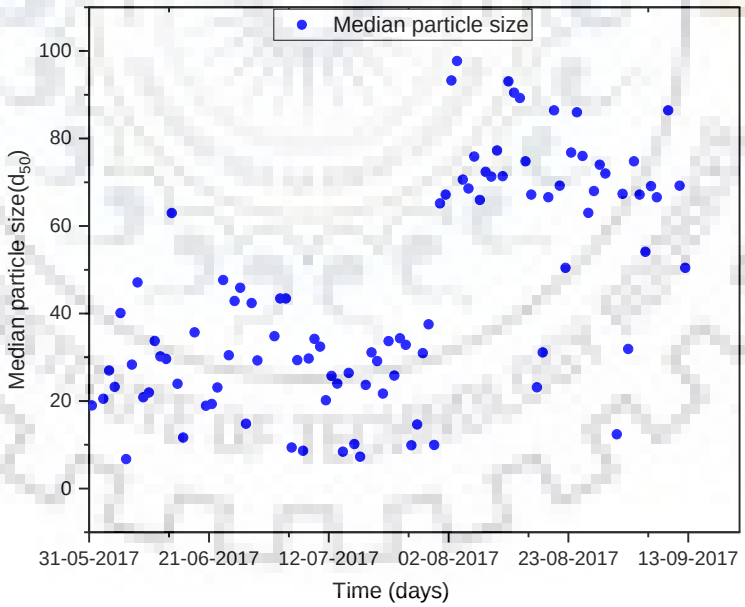

Figure 4.22: Median particle size (d_{50}) of the suspended sediment samples

It is observed from the graph that the median particle size of the graph varies from 6 µm to 90 µm in the forebay. The average particle size is found to be 46µm. It can also be seen that during the monsoon period, fine particles were transported through the turbine while coarser particle settle down at lower flow rate. More than 85% of the particles passing through the turbine falls in the range of 20 µm to 100 µm (between medium size silt and very fine sand)

as given in Table 4.2.

Table 4.2: Presence of Median size particle (d_{50}) in Sediment class

Sediment	Size class (μm)	Average range (%)
Medium silt	6-20	14.63
Coarse silt	20-63	54.8
Very fine sand	63-125	26.8

4.3.2 Suspended sediment concentration

Concentration is represented in the form of PPM (parts per million), which is equivalent to mg/litre or kilogram of particles in 1000m^3 of water (1000 ppm is equal to 0.1 percent), especially for river sedimentation. The LISST portable measures the mean size particle and volumetric concentration of the suspended sediment sample as shown in Figure 4.23.

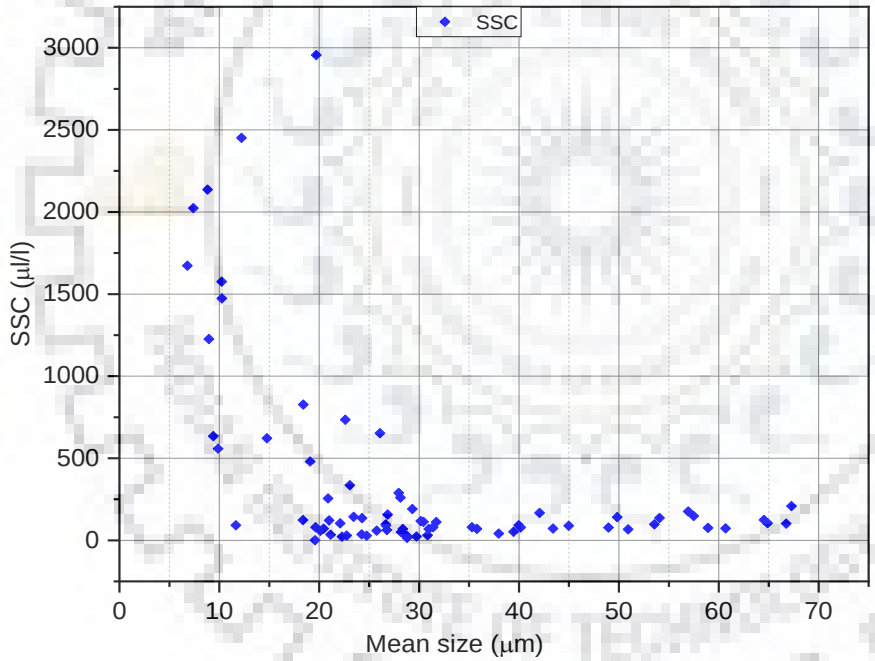

Figure 4.23: Plot between mean particle size and volumetric concentration

It is clear from the graph as shown in Figure 4.23 that most of the time volumetric concentration of samples varies from 50μl/l to 200μl/l whereas the average size of the particle varies from 18 μm to 70 μm which falls under the category of medium silt to fine sand particle size. The primary method to measure SSC is the gravimetric method. This involves filtering a known volume of sediment–laden water, drying the residue and weighing. The mass sediment concentration of samples were measured and analyzed from the graph plotted between time and total suspended sediments (TSS) measured in parts per million (ppm) as shown in Figure 4.24.

It is found during the study period that most of the time TSS remains under 200 ppm and in rainy days it has gone up to 3000 ppm.The particle concentration of the suspended sediment samples has not been increased beyond 3000 during the entire monsoon periods. Average mass sediment concentration of these samples comes around 215 ppm during study period.

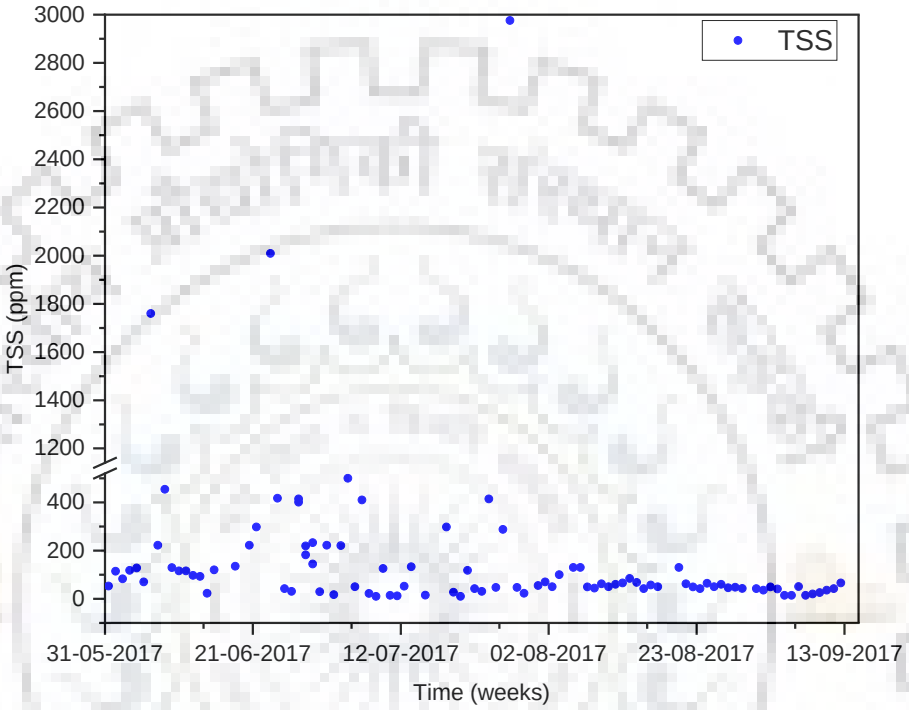

Figure 4.24: Particle concentration of suspended sediment sample

Turbidity of n = 50 manual samples were measured in the laboratory using Hach Portable Turbiditimeter (2100 P). The volumetric sediment concentration of manual collected samples from study sites was measured by using LISST portable instrument. LISST portable is linked with turbidity (NTU), as shown in Figure 4.25. A good relationship between turbidity ($\mathbf{R^2}$ = 0.95) and volumetric sediment concentration was discovered. This shows that at the study site, LISST is suitable for measuring SSC with an advantage in measuring median particle size.

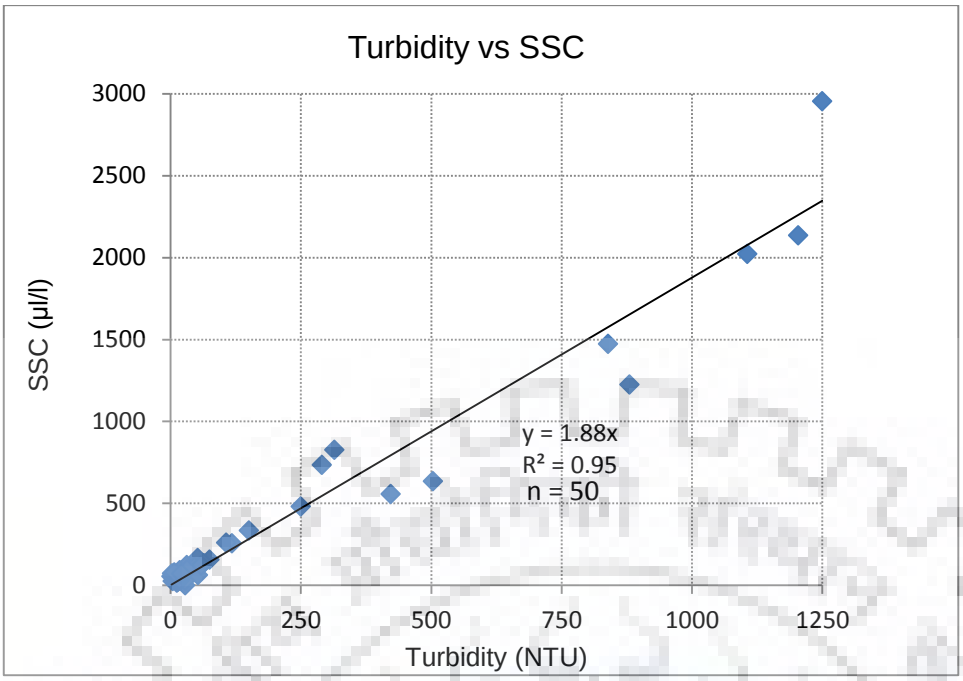

Figure 4.25: Plot between Turbidity and SSC measured from study site

4.3.3 Sediment shape

Scanning electron microscope (SEM) photographs of dried sediment sample were taken at different magnification as suggested in IEC 62364[9], the shape of the particles were found to be from angular to sub angular with grains of quartz, feldspar and lithic fragments by visualizing photographs taken under different magnification as shown in Figure 4.26, Figure 4.27 and Figure 4.28 respectively. However IEC-62364 recommends the value of shape factor (K_{shape}) for hydro-abrasive erosion as 1, 1.5 or 2 for round, sub-angular and angular particles respectively [9]. Therefore the value of shape factor considered for calculating particle load as 1.5 (sub-angular particle geometry).

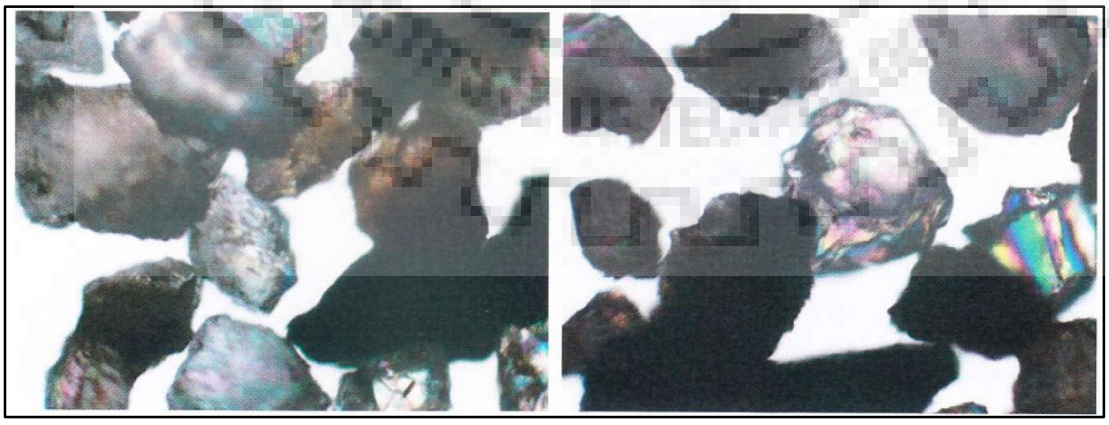

Figure 4.26: Mag=100x: Angular to sub-angular grains of quartz, feldspar and lithic fragments.

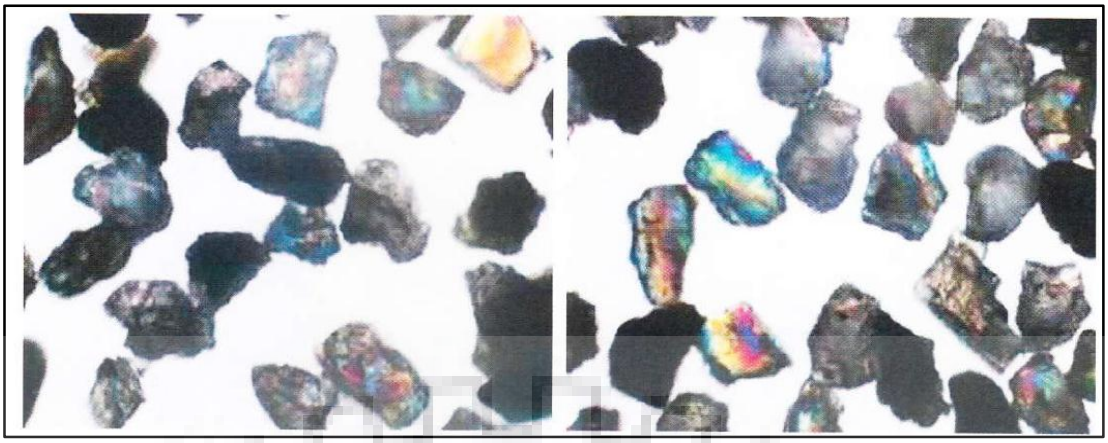

Figure 4.27: Mag=40x: Angular to sub-angular grains of quartz, feldspar and lithic fragments

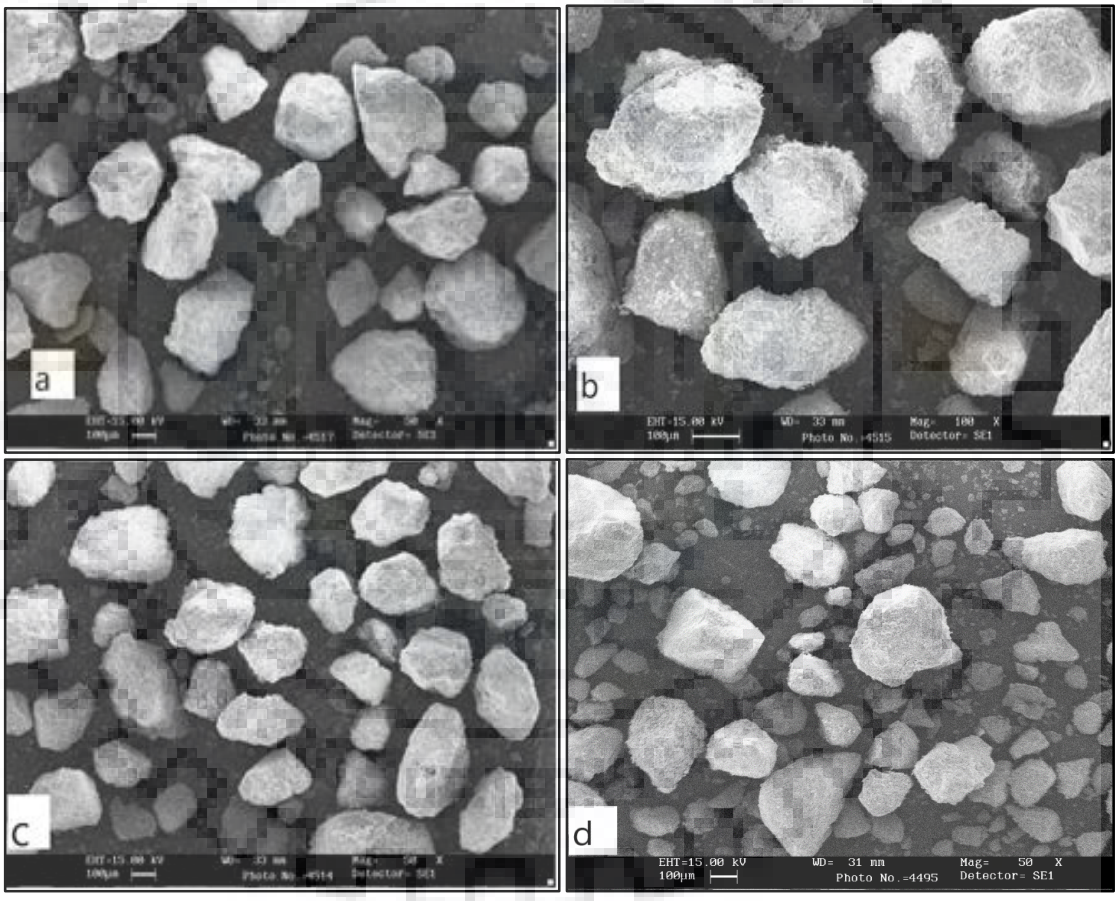

Figure 4.28: SEM photographs under different magnification of dried sediment samples of Forebay of CHEP-I.

4.3.4 Mineral content and Hardness

The mineralogical composition of sediment sample is carried out using X-ray diffraction which is nondestructive and analytical technique primarily used to identify different phases in crystalline material. The different phases present in sediment sample as provided in Figure 4.29.

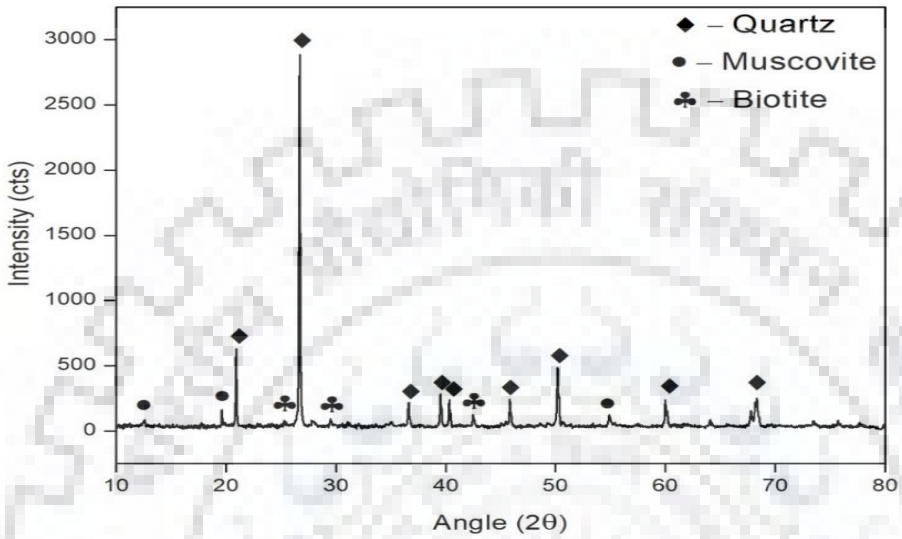

Figure 4.29: X-ray diffraction analysis of sediment sample from study site

Petrography is a quantitative approach to know about the detailed description of rocks like haredness, composition and shape etc.When seen under microscope, it was observed that the sediment particle comprise of quartz, feldspar, mica (muscovite and biotite, hornblende and magnetite. Quartz grains are angular to sub angular in shape where feldspar grains appear sub angular to angular. A few grains of the quartz are iron coated. Table 4.3 represents the various minerals identified, their hardness (H, as per Moh's scale) and standard specific gravity.

Table 4.3: Mineralogical composition of suspended sediments (in %) collected from study site

Minerals	Percentage	Hardness(on Moh's scale)	Specific gravity
Quartz	70-72	7	2.65
Feldspar	12-14	6	2.57
Hornblende	4-6	5.5	3.05-3.47
Mica	5-7	2.5-4	2.7-3.0
Magnetite	4-6	5.5-6.5	4.9-5.2

X-ray fluorescence is an analytical technique to determine the elemental composition in percentage of dried sediment sample. It gives an idea of percentage of each element present in the sample. It can be concluded from the Table 4.4. that silica is present in abundant

followed by calcium, aluminum and Iron, This further confirms that quartz content is very high in sediment sample collected from site which is mainly responsible for quick erosion to turbine as its hardness is more than material of turbine on Mohs scale.

Table 4.4: Percentage of elements of sediment dry sample

Name of Chemical	Symbol	Percentage (%)
Silica	Si	28.22
Calcium	Ca	7.049
Aluminum	Al	5.896
Iron	Fe	4.008
Potassium	K	2.423
Magnesium	Mg	0.7245
Titanium	Ti	0.40
Sodium	Na	0.3518
Manganese	Mn	0.1319
Phosphorus	P	0.0687

4.4 ESTIMATION OF EROSION RATE AND EFFICIENCY

Erosion can be quantified as erosion depth per unit time (µm/ h) assuming homogeneous erosion in a certain zone. It can also be quantified as gravimetric erosion rate in terms of mass loss per unit time referring to a certain point of time. The quantification and modelling of erosion is a complex phenomenons it depends on number of relevant and interdependent parameters. Sometimes the impact parameters resulting from the flow are not fully known. In engineering practice, the empirical relations are of great importance as they can be implemented easily. Such empirical equations are limited to specific application and comprise typically same parameters obtained from laboratory investigation and measurement at prototypes.

As per IEC- 62364, typical erosion damages of Pelton turbine are needle tips and seat rings, runner buckets, jet deflector, nozzle shields, Inner side of runner housing, grating below the runner. However the most affected parts of Pelton turbines are runner buckets, nozzle and its rings. The damage of both the parts due to sediment erosion increases the erosion rate which in turn changes the profile and hence reduces the efficiency of the turbine. There are various erosion models which have been developed by the researchers to estimate the erosion rate and efficiency reduction of the turbine.

4.4.1 Using International Electro Technical Commission (IEC) – 62364 (2013)

The technical committee of IEC has prepared a guide for dealing with hydro-abrasive erosion in different turbines which serves to present data on particle abrasion rate on several combinations of water quality, operating conditions, component materials and component properties collected from hydro site. It is assumed in this guide that cavitation is not present in the turbine and water is not chemically aggressive. The definitions of parameters along with symbols are given in Table 4.5.

Table 4.5: Symbols, Terms and Values suggested for IEC- 62364 to obtain erosion depth.

Symbol	Definition/Nomenclature as per IEC 62364	Values suggested
Δt	Exposure period [h]	2448 hours
Δde	Depth of erosion [mm] during Δt	to be find out
K_f	Coefficient reflecting the flow pattern, i.e. angle of attack and turbulence.A constant for each turbine component	1.76×10^{-5} for splitter height reduction, 2.99 x 10-5 for erosion in cut-out region and 5.43×10^{-6} and erosion depth in bucket outlet. [34]
RS	Reference size (length) of a turbine [m]; for Pelton turbines RS = inner bucket width B.	B = 0.334 m(from runner drawing)
p	Exponent, intended to be a constant for each turbine component, for consideration of curvature-dependent effects.	0.1458 For splitter height reduction, -0.0380 for erosion in cut-out region and 0.2959 and erosion depth in bucket outlet. [34]
k_m	Coefficient for the material at the surface of a turbine part, Km = 1 for martensitic stainless steel with 13% Cr and 4% Ni; Km < 1 for coating material;	0.12 [34]
w	Characteristic relative velocity [m/s] between the flow and the turbine part. $w = 0.5\sqrt{2gh}$; $g = 9.81\ m/s^2$ & $h =$ 365 m	42.31 m/s
x	Exponent ,varies from 3 to 4, IEC suggests value as 3.4	3.4 [7]
K_{size}	Coefficient for particle size, IEC suggests $K_{size} = d_{50}/1000$ µm (with d_{50} in µm)	46µm, (as discussed in para 4.3.1)
SSC	Suspended sediment mass concentration [g/l] = [kg/m^3], for Pelton turbines SSC = 0 if no flow	215 ppm (as discussed in para 4.3.2)
K_{shape}	Coefficient for particle shape, IEC suggests K_{shape} = 1 for rounded, 1.5 for sub angular or 2 for angular.	1.5 (as discussed in para 4.3.3)
$K_{hardness}$	Coefficient for particle hardness with respect to the hardness of the surface material, IEC suggest to take the mass fraction of particles harder than the surface material.	0.72, (as discussed in para 4.3.4)

4.4.1.1 The concept of Particle load

Suspended sediment concentration (SSC) and total suspended sediment load (SSL) are widely used to relate the sediment parameters to hydro-abrasive erosion; however, these parameters do not take into consideration the size, shape and mineral structure for corrosion. For this purpose, IEC 62364 (2013) adopted a new parameter as particle load (PL) to relate different sediment parameters to erosion. The integral of the product of particle related factors over

the exposure period is termed 'Particle load' (PL). PL reflects the cumulated erosion potential of the particles (at unit velocity) passing through a turbine as function of time. It is measured in (Kg.h/m^3). In contrast to SSL, the PL is not function of discharge and does not depend on the turbine design flow. The formula to calculate Particle load is given in Equation (4.2).

$$PL = \sum_{n=1}^{N} \left(C_n \times K_{\text{size,n}} \times K_{shape,n} \times K_{hardness,n} \times T_{s,\text{n}} \right) \quad (4.2)$$

where

C_n is the mass SSC in kg/m^3 for each sample;

K_{size} is the numerical value of median particle size, d_{50} in mm.

K_{shape} is shape factor of the particle geometry.

$K_{hardness}$ is the same numerical value as the fraction of particles harder than Mohs 4.5.

$T_{s,\,n}$ is the time interval to consider for each interval.

N is number of samples.

4.4.1.2 Adaptation of the PL for Pelton runners

In comparison to reaction turbines or nozzles of Pelton turbines, the erosion on a Pelton bucket is an intermittent process which means it take place during only a part of the operation time. The impact of erosion on a bucket decreases proportionally to the number of buckets Z_2 due of the shorter exposure time per bucket. On the other hand, the erosion enhances approximately proportional to the number of jets Z_0 because more buckets are simultaneously in contact with the sediment-laden water. The PL factor is modified as per Felix [33] is given in Equation (4.3).

$$PL_b = (Z_0/Z_2)\,PL \quad (4.3)$$

Where,

PL_b is the modified PL for bucket

Z_0 is the no. of jets

Z_2 is the no. of buckets

4.4.1.3 Erosion depth

The numerical value of erosion depth at different regions of Pelton bucket is calculated using the formula given in IEC-62364 [7] and is shown in Equation (4.4)

$$S = W^{3.4} \times PL_b \times Km \times K_f/RS^P \quad (4.4)$$

Where,

W is characteristic relative velocity [m/s] between the flow (or the particles) and the turbine part.

PL_b is modified particle load for bucket

Km is coefficient of turbine material constant

K_f is coefficient reflecting the flow pattern.

RS is reference size of the bucket

p is value of exponent for consideration of curvature dependent effects.

4.4.2 Using available correlations

The sediment laden water carries a lot of suspended sediment having different properties like size, concentration, shape and mineral content. When these sediments passed through the nozzle with high velocity of flow, it erodes the surface of the spear as well as seat rings. A case study of Chilime hydropower plant located in Nepal was carried out in order to investigate sand erosion of double jet Pelton turbine nozzles and buckets by Bajracharya et al. [32].The Chilime Hydropower plant is Run-of-River (ROR) scheme which has two 11 MW units of double jet Pelton turbines making total plant capacity of 22MW. In their study, the primary and secondary data was collected from the field site. The dried as well as suspended sediment samples were collected and analyzed to know the different sediment properties like particle size and mineral content. The measurement of wear depth due to sand erosion and surface roughness of eroded needle were measured using stylus probe in the laboratory. The relation of erosion rate with sediment properties like size and mineral content were established using correlations and then efficiency reduction was also calculated with the help of correlations developed for hydropower plant having similar scenario.

4.4.2.1 Erosion rate

The erosion models or correlations developed by the researchers to relate the sediment parameters with sand erosion are dependent on site conditions. In the present study, the sediment parameters like median size particle and quartz content of CHEP-I were measured and analyzed in the laboratory from the suspended sediment sample collected from the site. The petrographic analysis of the sediment sample revealed that the quartz content was about 70 -72 percent. The correlations or equations developed by Bajracharya at different percentage of quartz for calculating erosion rate by taking average particle is shown in Equation (4.5) and (4.6) respectively.

When quartz content up to 60 %; Erosion rate $\propto$ a (size) ^{b} a =1199.8; b=1.8025 (4.5)

When quartz content up to 80 %; Erosion rate $\propto$ a (size) ^{b} a =1482.1; b =1.8125 (4.6)

Where, size is average particle size of sediment sample

a and b are constants.

4.4.2.2 Efficiency reduction

The surface of the component of turbine on which erosion takes place gets eroded due to which profile of the component gets deformed. This will increase friction which also enhances erosion rate and reduces the efficiency of turbine. Bajracharya et al. had developed a correlation between erosion rate and efficiency reduction which is shown in Equation. (4.7).

$$\text{Efficiency reduction} \propto a\,(\text{erosion rate})^{b} \quad (4.7)$$

Where, a=0.1522; b=1.6946

4.5 RESULTS OF EROSION RATE AND EFFICIENCY REDUCTION

The erosion rate and efficiency reduction of Pelton turbine using IEC erosion model and available correlations of erosion are estimated for chenani hydroelectric project-I and discussed in detail as follows:

4.5.1 Particle load

As per Equation (4.2); it is clearly understood that the erosion depth is proportional to SSC and the exposure time. Thus, the same erosion depth is expected when a turbine runs e.g. 500h at 0.3g/l or for 50h at 3g/l (with the same particle property) and the PL is same in both cases. It can be concluded from the graph as shown in Figure 4.30 that during the operation of 2448 hours, the turbine was exposed to particle load (PL) =18.96 kg.h/m^3. Therefore the Particle load for individual bucket of runner to be calculated using Equation (13), i.e. PL_b = (2/21)18.96 = 0.0995 x 18.96= 1.8 kg.h /m^3. The modified Particle load is used to estimate the erosion depth at different regions of individual bucket.

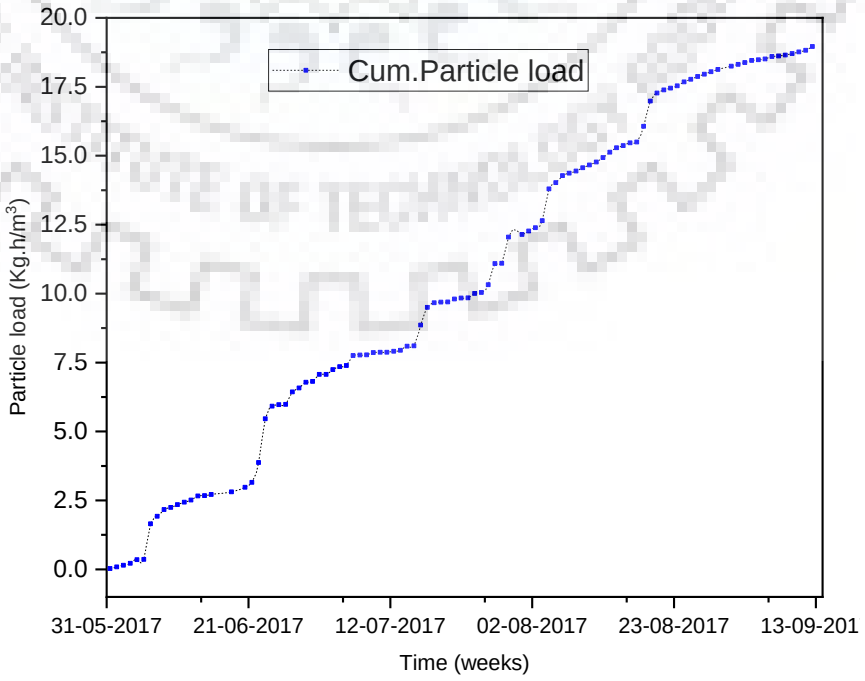

Figure 4.30: Cumulative Particle load graph.

4.5.2 Erosion depth of buckets

The estimated erosion depth for individual bucket using modified particle load for three different regions of runner bucket of Pelton turbine is given in Table 4.6.The particle load for individual bucket (PL_b) is calculated earlier using modified particle load equation. The value of coefficient reflecting the flow pattern (K_f) and exponent (p) for consideration of curvature dependent effect for three different regions of bucket is already discussed and also given in Table 4.5. The value of material constant k_m for martensitic stainless steel with 13% Cr and 4% Ni with HVOF coated is taken from literature [34].The reference size (RS) for the Pelton turbine bucket is the inner width of bucket whose value is 0.334 m. Therefore by using Equation (4.4); the erosion depth estimated is presented in the tabular manner for three different regions of runner bucket.

Table 4.6: Estimation of erosion depth of different component of Pelton bucket

Regions of Pelton bucket	w^x (m/s)	PL_b (kg.h/m^3)	k_m	k_f/RS^p	Erosion depth (mm)
Splitter height reduction	338825.5	1.8	0.12	0.00002	1.51
Erosion in cut-out region	338825.5	1.8	0.12	0.00003	2.10
Erosion depth in bucket outlet	338825.5	1.8	0.12	0.00001	0.55

It is clear from the Table 4.6 that erosion in cut-out region of the bucket was found to be 2.01 mm, splitter height reduction due to sand erosion was 1.45 mm and erosion depth in bucket outlet was 0.53 mm respectively. The photographs of Pelton runner were clicked during site visit and erosion of different regions of bucket is shown in Figure 4.31.

Figure 4.31: Images of Runner and eroded buckets of Pelton turbine of CHEP-I.

4.5.3 Erosion rate

The particle size of sediment sample of CHEP-I were analyzed during the study period and average particle size was determined. The average size of the particle came be 0.046mm.The erosion rate at 60 % quartz and 80% quartz were determined while considering 0.046 mm as average particle size. Then the average of these two erosion rates gave erosion rate at 70 % quartz content with average particle size. The graph was plotted between particle size and erosion rate at 70 % quartz content considering average size particle. It can be seen from the graph shown in Figure 4.32 that erosion rate of needle was found to be 5.099 mm with average particle size of 0.046mm during study period.

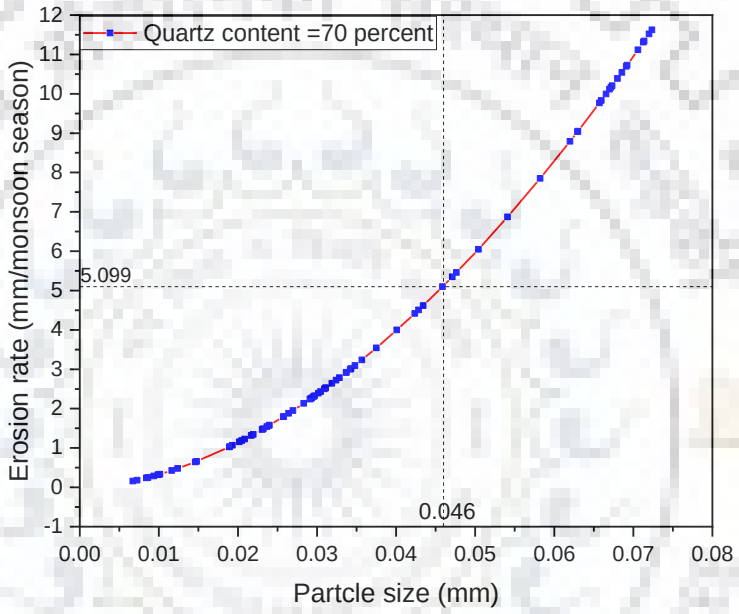

Figure 4.32: Plot between particle size and Erosion rate

4.5.4 Efficiency reduction

The surface profile or geometry of the components of turbine gets disturbed due to the effect of sand erosion. This will increase friction which also enhances erosion rate and reduces the efficiency of turbine. The relation between erosion rate and efficiency reduction as discussed already in Equation (4.7). The graph plotted between erosion rate and efficiency reduction as shown in Figure 4.33.

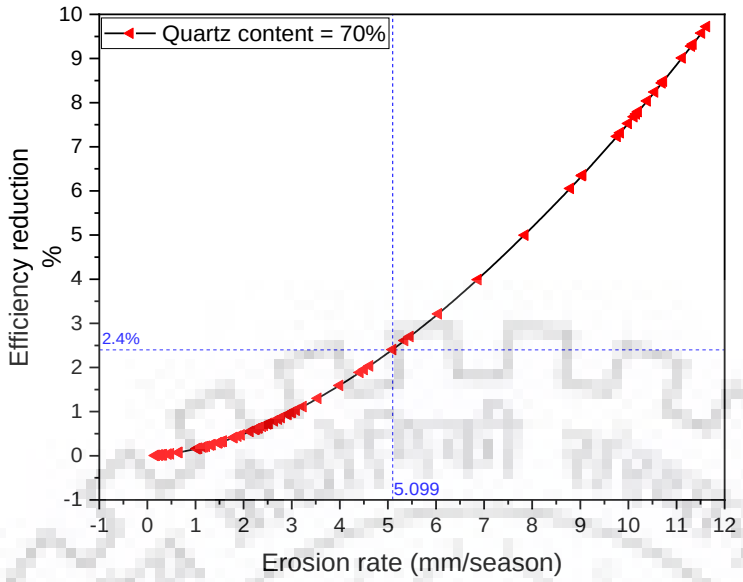

Figure 4.33: Plot between erosion rate and efficiency reduction.

Efficiency reduction of turbine is estimated considering erosion rate equals to 5.099 mm taking 70 % quartz content into consideration during study period. The efficiency reduction of turbine during this period came to be as 2.4 % which would have direct impact on loss of generation due to sand erosion. The photographs of needle of the upper nozzle system of unit 1 were clicked before and after monsoon period is shown in the Figure 4.34. It was found out during the monsoon the height and weight of needle gets reduced due to adverse impact of sand erosion.

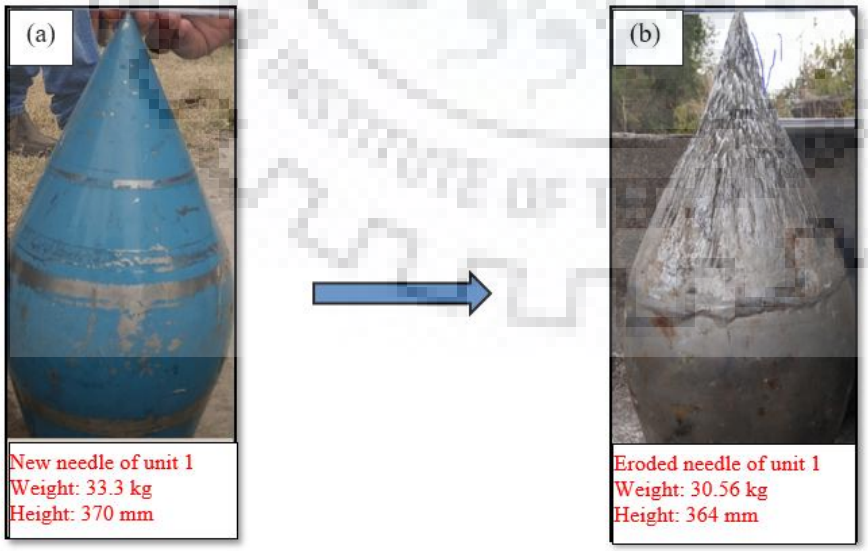

Figure 4.34: Photographs of needle of unit 1 (a) before monsoon (b) after one monsoon season.

4.6 MEASUREMENT OF EROSION AT SITE

During the study period, the site was visited frequently to study various component of Power plant, for collection of sediment samples, to get primary as well as secondary data and to measure the components of turbine. After monsoon period, when the nozzle of turbine was opened to replace damaged components with new one. The photographs of upper nozzle system of twin jet Pelton turbine during the operation of the turbine is provided in the Figure 4.35. The initial measurement of new spear and seat ring before monsoon have been recorded as shown in Figure 4.36. After monsoon period, when the nozzle of turbine was opened to replace damaged components with new one. The eroded spear and seat ring were measured again as shown in Figure 4.37.

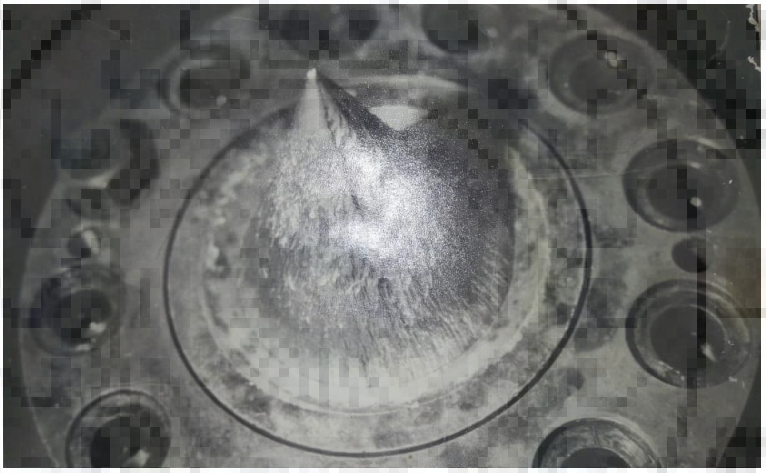

Figure 4.35: Upper nozzle system of twin jet Pelton turbine of CHEP-I.

(a)Spear and seat ring of machine unit 1

(b) Top view of spear and seat ring

(c) No gap between spear and seat ring

(d) Measurement of height spear of machine unit I

(e) Measurement of weight of of spear on weigh machine

(f) Specification of Spear of unit 1

Figure 4.36: Photographs of spear and seat ring of machine unit 1 of CHEP-I before monsoon season.

Figure 4.37: Photographs of spear and seat ring of machine unit 1 of CHEP-I before monsoon season.

The height of needle measured with steel measuring tape before monsoon was 370 mm and after one monsoon season, the height of the needle was found to be 364 mm. It can therefore be said that the needle height is lowered by 6 mm owing to erosive wear, which is in good comparison to the predicted erosion rate using available erosion correlation developed so far. The initial and final needle weight was also evaluated using an electronic weighing machine and the needle mass loss owing to sand erosion was found to be 2.74 kg.

CHAPTER 5
CONCLUSIONS AND RECOMMENDATIONS

5.1 CONCLUSIONS

Sand erosion in turbines has become a major issue in hydropower plants as the river carries a lot of sediments along with discharge. The problem of sediment erosion is more severe in Run-of-River scheme based high head turbines (Pelton and Francis) during monsoon. The performance of Pelton turbine decreases due to sediment erosion. Pelton buckets and nozzles are the parts which mainly got affected when the suspended sediments passes through these components.

In the present study, an attempt has been made to relate suspended sediment properties like concentration, Particle size, shape and mineral hardness and operating conditions with available erosion models to estimate the erosive wear as well as efficiency drop in different parts of Pelton turbine. For this, a field study has been conducted in Run-of-River based high head Chenani Hydroelectric project-I (5 x 4.66 MW) to investigate the problem of sand erosion in twin jet horizontal Pelton turbine of 4.66 MW. Based on investigations, following conclusions are drawn

i. During the study period, it was found that more than two third of sediment particle transported in Tawi River falls in the range of 6 microns to 125 microns (between medium size silt and very fine sand),sub angular to angular in shape with high quartz content. These sediments are reported to be highly erosive to turbine components and should be prevented from entering the machine unit as to increase the longevity of turbine components.

ii. The mass sediment concentration of samples measured using gravimetric method have not gone beyond 3000 ppm during the entire study period. It has been observed that during the monsoon period, sand particle concentration increases drastically from the average value and during non-monsoon, the particle concentration remained under 150 ppm which is less than the average value.

iii. Petrography of the dried sediment sample has been carried out and presence of quartz (70-72 %), feldspar (12-14%), mica (muscovite and biotite, hornblende and magnetite.) has been found. More than 85 % of minerals of incoming sediments were harder than material of turbine. The Pelton turbine installed in the power plant was made up of 13Cr-4Ni martensitic steel which has hardness of 4.5 on Mohs scale. X-

ray fluorescence has also been carried out to find the percentage of elements in the sediment samples. Silica (28%), Calcium (7.049 %), Aluminum (5.896%), Iron (4.008%) are found in the sediments.

iv. Scanning electron microscope (SEM) photo micrographs of the dried sediment sample under different magnifications were taken and found that quartz grains varied from angular to sub angular in shape where feldspar grains appear sub angular to angular. A few grains of the quartz are iron coated. Visualization of various photographs taken under different magnification shows that most of the time particle shape remained sub-angular and the value of shape factor is 1.5 for sub-angular particle geometry.

v. Erosion models developed by International electro technical commission (IEC)-62364 and researchers like Bajracharya , have been studied thoroughly and used to estimate erosion depth and efficieciency drop of Chenani Hydroelectric project-I. Erosion depth of the regions of bucket like Splitter height reduction, erosion in cut-out region and erosion depth in bucket outlet was estimated using IEC-62364 and it was found to be 1.51mm, 2.10 mm and 0.55 mm respectively. During the turbine operation of nearly three and half month, it was exposed to particle load of 18.107 kg.h/m^3.

vi. Correlations developed in earlier study were used to estimate the erosion rate and efficiency reduction of the nozzle of Pelton turbine installed at Chenani hydroelectric project-I. Erosion rate of 5.1mm/monsoon season of nozzle and efficiency reduction of 2.4 % have been estimated. The measurement of nozzle erosion rate at site was found to have a good relation in comparison to the estimated erosion rate.

5.2 RECOMMENDATIONS

The issue of sand erosion in hydro turbines is one of the main operation and maintenance problems that need to be addressed during the planning, construction, repair and maintenance of hydropower projects specially installed on high sediment laden rivers.

There is a need to develop erosion models based on actual flow conditions as to relate sediment parameters with erosion rate as well as efficiency reduction in Pelton turbine. Latest sediment monitoring techniques and equipments should be used to measure and analyze the sediments and erosion depth. A Techno economic analysis are required to be carried out and correlation needed to be developed between turbine erosion, efficiency changes, cost of repair and maintenance, cost of preventive maintenance based on field data. These may proove beneficial for hydropower developers to decide about the replacement of components of turbines without compromise with efficiency of the power plant.

PUBLICATIONS

Sharma, A. and Saini, R.P., Effect of sand erosion on Pelton turbine: a case study of Chenani Hydroelectric Project-I, J&K, India, ISH Journal of Hydraulic Engineering, (communicated).

REFERENCES

[1] International Hydropower Association, (2018).Hydropower status report, sector and insights.

[2] Hydro-Abrasive Erosion Issues in Indian Hydropower plants, Workshop on Abrasive erosion in Hydro Plants, Feb23-24 (2018), IIT Roorkee.

[3] www.mechanicalbooster.com/2016/10/pelton-turbine-working-main-parts-application -with-diagram.html (accessed on 22 Nov. 2018).

[4] wwww.renewablesfirst.co.uk/hydropower/hydropower-learning centre/Cross flow turbine. (accessed on 22 Nov. 2018).

[5] www.renewablesfirst.co.uk/hydropower/hydropower-learning-centre/Crossflow turbine. (accessed on 22 Nov. 2018).

[6] www.mechanicalboosters.com/2018/01/ turbine.html. (accessed on 23 Nov. 2018).

[7] Padhy M.K. (2009), Study of silt erosion on Pelton turbine for a small hydropower plant, Ph.D. thesis. IIT Roorkee.

[8] Sangal, S., Singhal, M.K. and Saini, R.P., 2018. Hydro-abrasive erosion in hydro turbines: a review. International journal of green energy, 15(4), pp.232-253.

[9] IEC 62364 (2013), Guide for dealing with hydro-abrasive erosion in Kaplan, Francis and Pelton turbine.Editon 1.0 International electro technical commission (IEC) Geneva, Switzerland.

[10] Rai, A.K., Kumar, A. and Staubli, T., 2017. Hydro-abrasive erosion in Pelton buckets: Classification and field study. Wear, 392, pp.8-20.

[11] www.sciencedirect.com/science/article/pii/S0043164817306506.(accessed on 25 November 2018).

[12] Chitrakar S., Neopane H.P. and Dahlhaug O.G. (2018), A Review on sediment Erosion Challenges in Hydraulic Turbines, Chapter, April 2018, DOI: 10.5772/intechopen.70468.

[13] Padhy, M.K. and Saini, R.P., 2012. Study of silt erosion mechanism in Pelton turbine buckets. Energy, 39(1), pp.286-293.

[14] Felix, D. (2017).Experimental investigation on suspended sediment, hydro-abrasive erosion and efficiency reductions of coated Pelton turbines. Ph.D. Thesis, Civil, Environmental and Geomatic Engineering Department, ETH Zurich, Switzerland.

[15] Thapa, B.S, Thapa, B., & Dahlhaug, O.G (2012).Current research in hydraulic turbines for handling sediments. Energy, 1-8.

[16] Bushan.B, Introduction to tribology, John wiley & sons, New York, emphasize the material displacement on a given body, with no net change in weight or volume

also should be consider as wear.

[17] Stachowiak G.W. and Batchelor A. W., 1993. Engineering Tribology, Elesevior, Amsterdam.

[18] Bjordal M. (1995), Erosion and corrosion of ceramic-metallic coatings and stainless steel, Dr. Ing. Thesis, Universitetet I Trondheim, NTH.

[19] Hojo H., Sudaand K.T and Yabu TT. (1986) Erosion damage of polymeric material by slurry, Wear (112) pp 17-28.

[20] Rai A. and Kumar. A (2017), Sediment monitoring for hydro-abrasive erosion: A field study from Himalayas, India, International Journal of fluid machinery and systems. Journal 0(2):146-153.

[21] Sheldon, G.L. and Finnie, I., 1966. On the ductile behavior of nominally brittle materials during erosive cutting. Journal of Engineering for industry, 88(4), pp.387-392.

[22] Bahadurand S. and Badruddin R., (1990), Erodent particle characterization and the effect of particle size and shape on erosion, Wear (138) 189-208.

[23] Chen Q., Li D. Y. (2003), Computer simulation of solid particle erosion, Wear (254) pp 203- 210.

[24] D.K. Lysne, B.Glover, H. Stole, E. Tesaker, Hydropower development book series number-8Hydraulic design, NTNU 2003.

[25] Rai, A.K. and Kumar, A., 2018. Measurements and financial analysis for hydro-abrasive erosion in hydropower plants. IASH Journal-International Association for Small Hydro, 7(1), pp.3-10.

[26] Padhy, M.K. and Saini, R.P., 2008. A review on silt erosion in hydro turbines. Renewable and Sustainable Energy Reviews, 12(7), pp.1974-1987.

[27] Padhy, M.K. and Saini, R.P., 2012. Study of silt erosion mechanism in Pelton turbine buckets. Energy, 39(1), pp.286-293.

[28] Truscott, G.F., 1972. A literature survey on abrasive wear in hydraulic machinery. Wear, 20(1), pp.29-50.

[29] Bardal, E., 1994. Korrosjon og Korrosjonsvern. Tapir.(in Norwegian).

[30] Tsuguo (1999), Estimation of repair cycle of turbine due to abrasion caused by suspended sand and determination of desilting basin capacity. In: Proceedings of international seminar on sediment handling technique, NHA, Kathmandu.

[31] Padhy, M.K. and Saini, R.P., 2011. Study of silt erosion on performance of a Pelton turbine. Energy, 36(1), pp.141-147.

[32] Bajracharya T.R., Acharya B., Joshi C.B, Saini R.P, O.G Dahlhaug(2008), Sand erosion of Pelton turbine nozzles and buckets: a case study of Chilime hydropower

plant. Wear 2008; 264:177–84.

[33] Felix. D, Abgottspon. A, Albayrak. I and Boes. R.M (2016), Hydro-abrasive erosion on coated Pelton runner: Partial calibration of IEC model based on measurement in HPP Fieschertal, IOP, conference ser: earth and environment. Sci.4.9 122009.

[34] Rai, A.K. (2017) Hydroabrasive erosion in Pelton turbine, Ph.D. Thesis. Alternate Hydro Energy Centre, IIT Roorkee, India.

[35] Padhy, M.K. and Saini, R.P., 2009. Effect of size and concentration of silt particles on erosion of Pelton turbine buckets. Energy, 34(10), pp.1477-1483.

[36] Thapa B. (2004), Sand erosion in Hydraulic machinery. PhD thesis. NTNU, Norway.

[37] Krause M., Grein H. (1996), Abrasion Research and Preventation, Hydropower Dams (4), 7- 20.

[38] www.sympatec.com/en/particle-measurement/sensors/laser-diffraction (accessed on 5 April 2019).

[39] Kumar S. Development displacement and human right violation in India with special reference to Jammu and Kashmir, a case study on Baglihar dam. Int J Multidiscipline Res Social Manag Sci 2014; 2(1):104–8.

[40] Sharma, A.K. and Thakur, N.S., 2017. Assessing the impact of small hydropower projects in Jammu and Kashmir: A study from north-western Himalayan region of India. Renewable and Sustainable Energy Reviews, 80, pp.679-693.